DISSERTATION

submitted to the
Combined Faculties for the Natural Sciences and for Mathematics
of the Ruperto-Carola University of Heidelberg, Germany

for the degree of

Doctor of Natural Sciences

presented by

Başak Özata, Doctor of Veterinary Medicine

born in Ankara, Turkey

Oral-examination

.....

Functional and Kinetic Studies of COPI Machinery

Referees:

Prof. Dr. Felix Wieland

Prof. Dr. Walter Nickel

Anneme ve Babama..

Table of contents

Abstract

In this study, different aspects of vesicular transport in the early secretory pathway have been investigated.

Although an earlier study showed an effect upon the down regulation of β-COP in the transport of the SH4 domain containing HASPB and Yes (Ritzerfeld et al., 2011), there was no study revealing the role of coatomer subunits in plasma membrane localization of unconventionally secreted proteins. This work investigates the role of γ2-COP in the transport of the unconventionally secreted proteins HASPB and Yes. Pronounced retention of HASPB at the perinuclear region was observed after down regulation of the coatomer subunits α, β, δ, and ζ suggesting that the coatomer subunits and therefore most likely COPI vesicles are involved in the transport of HASPB. However individual knockdowns of γ1- and γ2-COP subunits did not affect the transport of the reporter proteins, indicating there is no specific role of coatomer isoforms *per se*.

In the second part, the impact of novel Brefeldin A (BFA) analogs on the Golgi morphology was investigated. Treatments of mammalian cells with various analogues revealed that number of derivatives had no impact on the Golgi morphology in given times in addition to some derivatives causing reversible Golgi disruption as Brefeldin A. The variation of the effect can be of use in various fields for creating new therapeutics.

Another part of this work focusing on the oligomerization of the p24 protein and a non-SM18 binding p24 variant (L17F) were studied by cross-linking the proteins *in vivo* using a chemical cross-linking agent. This shows a significant reduction in the oligomeric form of the non-SM18 binding p24 variant compared to the monomeric form.

The final part of this thesis presents the findings on the kinetics of p24 family members using Fluorescent Loss in Photobleaching (FLIP). Experiments

resulted in no significant differences between transport rates of p23 and p24 from the Golgi to the endoplasmic reticulum.

Zusammenfassung

Im Rahmen dieser Arbeit wurden verschiedene Aspekte des vesikulären Transports im frühen sekretorischen Weg untersucht.

Obwohl frühere Arbeiten die Auswirkung der Herunterregulierung von β-COP auf den intrazellulären Transport von SH4-Fusionsproteinen (Ritzerfeld et al., 2011) zeigen, gibt es keine Untersuchungen bezüglich der Rolle von Coatomer Untereinheiten bei der Plasmamembranlokalisierung von unkonventionell sezernierten Proteinen. In dieser Arbeit wurde die Rolle von γ2-COP beim Transport der unkonventionell sezernierten Proteine HASPB und Yes untersucht. In Folge der Herunterregulierung der Coatomer Untereinheiten α, β, δ und ζ konnte eine deutliche Retention von HASPB in der perinukleären Region festgestellt werden. Das deutet darauf hin, dass diese Coatamer Untereinheiten und somit COPI-Vesikel am Transport von HASPB beteiligt sind. Allerdings hatte der einzelne Knock-down von γ1- und γ2-COP Untereinheiten keinen Einfluss auf den Transport der Reporterproteine. Dies weist darauf hin, dass die Coatomer Isoformen an sich keine spezifische Funktion bei dieser Art von Transport haben.

Zudem wurden neuartige Brefeldin A (BFA)-Analoga hinsichtlich ihres Einflusses auf die Morphologie des Golgi-Apparates untersucht. Es konnte gezeigt werden, dass einige Derivate keinerlei Wirkung auf die Golgi-Morphologie haben, wogegen andere wie BFA einen reversiblen Zerfall des Golgi-Apparates verursachen. Die Bandbreite der unterschiedlichen Effekte kann in verschiedenen Einsatzbereichen genutzt werden, um neue Therapeutika herzustellen.

Des Weiteren wurde *in vivo* die Oligomerisierung des p24-Proteins und einer p24-Variante, die die Sphingomyelinspezies (SM18) nicht mehr bindet (L17F), mittels chemischer Quervernetzung untersucht. Diese Studien zeigten eine erhebliche Abnahme der oligomeren Form der p24-Variante im Vergleich zur monomeren Form.

Im letzten Teil dieser Arbeit werden die Ergebnisse bezüglich der Kinetik der p24-Familienmitglieder unter Verwendung von *Fluorescent Loss in Photobleaching* (FLIP) vorgestellt. Dabei zeigten sich keine signifikanten Unterschiede zwischen p23 und p24 bezüglich ihrer Transportraten vom Golgi zum Endoplasmatischen Retikulum.

1. Introduction

A hallmark of eukaryotic cells are their characteristic membrane structures in the cytoplasm. These membrane enclosed organelles are necessary for specific metabolic activities that are vital for the cell. The specific compositions of these organelles are conserved although there is a continuous molecular exchange between the organelles within a cell. Protein and lipid homeostasis in eukaryotic cells depends on many cellular processes, including highly regulated transport between the membrane bound compartments carried out by conventional and unconventional secretion. The majority of newly synthesized cargo follows the secretory pathway in transport vesicles, starting at the Endoplasmic Reticulum (ER), followed by the Golgi apparatus and from there to its final destination in the cell. However, quite a number of proteins are secreted without entering this pathway or bypassing organelles on the way, which has been termed unconventional secretion (Rabouille et al., 2012).

1.1. Conventional secretory pathway

The classical secretory pathway in the cell begins at Endoplasmic Reticulum and the cargo is directed from ER to plasma membrane, endosomal-lysosomal system or other organelles. Throughout the secretory pathway in eukaryotic cells, a variety of coated vesicles are responsible for the delivery of cargo. They are also involved in sorting mechanisms at the membrane, which is important to maintain the composition of the organelles (Bonifacino and Glick, 2004; Cottom and Ungar, 2012). In the early part of the secretory pathway, between ER and Golgi, vesicular transport occurs bidirectionally; Coat Protein Complex II coated (COPII) vesicles are responsible for anterograde transport from ER to Golgi and Coat Protein Complex I coated (COPI) vesicles mediate the retrograde transport from Golgi to ER as well as the bidirectional transport within the Golgi apparatus (Nakano et al., 2009; Sato, 2004).

1.1.1. COPII coated vesicles

Biogenesis of the COPII vesicles begins with the activation of a small GTPase: Sar1. Sar1 acts as a molecular switch between inactive GDP-bound state to active GTP-bound state and this switch is controlled by Guanine Exchange Factors (GEF) (Adolf et al., 2013). Active Sar1 binds to a Sec23/Sec24 dimer, which is a heterodimeric subcomplex of the COPII coat (Szul and Sztul, 2011). Subsequently, the Sec13/Sec31 heterotetrameric complex is recruited to the Sec23/24 part of the coat (Farhan and Rabouille, 2011; Lee et al., 2004), which induces coat polymerization that leads to the formation of a vesicle (Hicke et al., 1992; Matsuoka et al., 1998; Salama et al., 1993). In addition to the minimal machinery, COPII vesicles contain newly synthesized cargo to be transported to the Golgi for further processing and maturation (Hirschberg and Lippincott-Schwartz, 1999). Sorting of the cargo occurs at the ER exit sites (ERES), where the sorted cargo, further targeting molecules (v-SNARE (vesicle-soluble NSF (N-ethylmaleimide-sensitive factor) attachment protein receptor)) (Campbell and Schekman, 1997), and receptors (e.g. p24 proteins) are concentrated and later form COPII vesicles (Zanetti et al., 2012).

1.1.2. COPI coated vesicles

The small GTPase Arf1 (ADP-ribosylation factor 1) initiates biogenesis of the COPI vesicles. Arf1-GDP is recruited in its inactive form to the Golgi membrane from the cytosol by the C-terminal tail of the p24 family members (Gommel et al., 2001). Arf1-GDP is then activated by the nucleotide exchange factor GBF1 (which was erroneously named Golgi-specific Brefeldin A resistant guanine nucleotide exchange factor 1) catalyzing exchange of GDP to GTP in Arf1. Upon GTP loading, Arf1 undergoes a conformational change and increases membrane binding by inserting its amphipathic helix into the membrane (Antonny et al., 1997; Niu et al., 2005). Arf1, together with p24 family members, recruits a soluble cytosolic heptameric complex termed coatomer to the Golgi membrane. Binding to p24 family members causes a conformational change and initiates the polymerization of coatomer (Reinhard et al., 1999). Subsequently, the polymerization of the coat protein causes membrane

deformation and COPI vesicles bud off from the membrane (Bethune et al., 2006). When COPI vesicles reach their target membrane, a first attachment occurs via tethering factors, followed by association of SNAREs between two membranes, which leads to fusion and the release of their content (Cottom and Ungar, 2012). Several reports indicate that the COPI system is involved in the homeostasis of lipids (Beller et al., 2008; Soni et al., 2009) as well as protein transport in the cell (Lippincott-Schwartz and Liu, 2006; Rothman and Wieland, 1996; Serafini et al., 1991b).

1.1.2.1. ADP-ribosylation factor 1(Arf1)

Arf1 is a small guanosine triphosphatase (GTPase) that mainly regulates vesicular traffic (Casanova, 2007; D'Souza-Schorey, 2006). Nucleotide exchange of Arf-GDP to Arf-GTP via GBF1 (Golgi-specific Brefeldin A resistant guanine nucleotide exchange factor 1) triggers a conformational change in Arf1, which then inserts its N-terminal myristoylated helix into the membrane (Antonny et al., 1997). This shallow insertion helps to create positive curvature at the membrane that eventually allows formation of a bud (Beck et al., 2008).

Nucleotide exchange factor GBF1 (in spite of its name) is known to be Brefeldin A sensitive. Brefeldin A is a unique fungal metabolite and has an unusual reversible effect on Golgi morphology. It causes a block of protein transport between ER and Golgi in eukaryotic cells (Fujiwara et al., 1988). Brefeldin A binds to a Arf-GDP-Sec7 domain complex (the first intermediate in the nucleotide exchange process) and prevents the exchange of GTP for GDP, thereby blocking the association of Arf with Golgi membranes and inhibition of COPI mediated transport (Claude et al., 1999; Donaldson et al., 1992; Helms and Rothman, 1992a; Peyroche et al., 1999). Additionally, Brefeldin A causes apoptosis and reduces proliferation of cancer cells, and is a topic of intensive research (Seehafer et al., 2013; Shao et al., 1996). Furthermore, BFA is known to be an inhibitor of enterovirus RNA replication in infected cells and to cause an assembly defect on Herpes Simplex Virus type1 (Cuconati et al., 1998; Dasgupta and Wilson, 2001).

As BFA is an important tool in different fields of research, analogues were synthesized in the anticipation of improved *in vivo* stability and solubility while rendering the compound less toxic for the cells. The cytostatic activity however should be maintained when compared to the original BFA (Förster et al., 2011b; Seehafer et al., 2013). Two separate batches of newly synthesized Brefeldin A analogues were tested for their biological properties in mammalian cells for their effect on Golgi morphology in this thesis (see Chapter II).

Recruitment of coatomer and stabilizing the complex at the membrane requires several interactions between Arf1, coat proteins and membrane proteins. Arf1 interaction with different coatomer subunits has been shown *in vitro* by site specific photo-crosslinking experiments to include β- and γ-COP as well as β'- and δ-COP (Sun et al., 2007; Zhao et al., 1997; Zhao et al., 1999). Furthermore, an interaction with ε-COP was found in two hybrid experiments (Eugster et al., 2000; Sun et al., 2007). *In vitro* crosslinking and Foerster resonance energy transfer (FRET) experiments in live cells reveals an interaction between C-terminal tails of the Arf1-GDP with dimeric members of the p24 family (Gommel et al., 2001; Majoul et al., 2001). These interactions stabilize coatomer at the membrane.

1.1.2.2. p24 family members

p24 proteins are a family of highly conserved type I transmembrane proteins with a molecular weight range of 24 kDa, and are important players in the early secretory pathway. The topological characteristics of these proteins are large N-terminal luminal domains, a single transmembrane segment and a cytoplasmically exposed short (12-20 amino acids) C-terminal tail. The latter allows the binding of the coat proteins I and II (Dominguez et al., 1998; Fiedler et al., 1996; Sohn et al., 1996).

The p24 family members were categorized and named differently, which also differs between species. As a result, various nomenclatures exist. According to phylogenetic clustering, they can be divided into four subfamilies, known as p24α, p24β, p24γ and p24δ, most of which exist in eukaryotic species

(Dominguez et al., 1998; Strating et al., 2009). The number of representatives of each subfamily differs across the species and typically 8-11 total members were found per genome (Dancourt and Barlowe, 2010; Strating et al., 2009). In this thesis, mainly two important members of this family will be examined: p23 and p24, which belong to the p24δ and p24β subfamilies, respectively.

Most p24 proteins form heterooligomers. This was shown by immune-precipitation: The p23 and p24 proteins form a complex and there is also efficient *in vivo* crosslinking (Fiedler and Rothman, 1997; Gommel et al., 1999; Jenne et al., 2002). Further studies show that there is a highly dynamic and complex interaction between the p24 family members except two of the subfamily members, p26 and tp24 (Jenne et al., 2002). In addition to monomeric and dimeric forms, p24 family members can form tetramers via their cytoplasmic domains and higher oligomeric forms were observed upon *in vivo* crosslinking via transmembrane domains (TMD) (Contreras et al., 2012; Jenne et al., 2002; Wiedler et al., 2000). Oligomerization of the family members is important for their correct localization and stability (Jenne et al., 2002). p24 dimers interact with γ trunk and appendage domains, which stabilizes coatomer on the Golgi membrane (Bethune et al., 2006; Harter and Wieland, 1998; Popoff et al., 2011a). Recently, in addition to the oligomerization of the p24 family members, an interaction of a specific lipid species, sphingomyelin (SM 18:0), and p24 was discovered. FRET experiments with fluorescent lipids revealed that lipid-protein interaction increases oligomerization of p24 and modulates the efficiency of COPI-vesicle mediated retrograde trafficking (Contreras et al., 2012). The oligomerization of p24 and a non-SM18 binding variant of the protein is investigated by *in vivo* crosslinking in Chapter III.

p24 family members cycle between the membranes of the early secretory pathway. Several functions, including COPI vesicle biogenesis, have been proposed (Gommel et al., 1999; Jenne et al., 2002): One proposed function is that of a cargo receptor. Deletions of the analog of p24 (Emp24p) in yeast have revealed a transport delay of the glycosylphosphatidylinositol (GPI)-anchored protein Gas1p (Schimmoller et al., 1995). A knockdown of p23 resulted in a delay of the plasma membrane expression of GPI-anchor proteins in general

and slowed down the maturation of a specific GPI-anchor protein: DAF (decay-accelerating factor). Other non-GPI-anchor proteins, however, were hardly affected. These data suggest that the transport of GPI-anchored proteins is regulated by p23 and p24 (Takida et al., 2008). p23 and p24 also work in the ER export of GPI-anchored proteins as cargo receptors by facilitating the ER export of these proteins depending on the interaction of certain Sec24 isoforms with p23-p24 complexes (Bonnon et al., 2010). p23 was, furthermore, shown to have a receptor function for coatomer at the Golgi membrane (Sohn et al., 1996) and p24 proteins were found as cargo receptors for Wnt proteins and required for their exit from ER (Buechling et al., 2011).

Members of the p24 family were proposed to contribute to the structural maintenance of the Golgi (Denzel et al., 2000) as well as to the formation of ER exit sites (Lavoie et al., 1999). Additionally, mutations of p24 proteins can influence structural organization of the ER and the Golgi apparatus (Aguilera-Romero et al., 2008; Lavieu et al., 2010; Mitrovic et al., 2008). Inactivation of one allele of p23 in mice causes structural changes in the Golgi structure (Denzel et al., 2000) and p23 was proposed to play a role to form and maintain the membrane structure of the *cis*-Golgi Network (CGN) (Rojo et al., 2000). However, in these reports, p23 was exogenously overexpressed, and it has been shown that overexpression of the p24 family members causes their mislocalization and accumulation at the ER. Therefore overexpression of p24 family members is prone to artifacts due to unphysiological localizations (Blum et al., 1999; Dominguez et al., 1998; Fullekrug et al., 1999; Rojo et al., 2000).

Genetic and biochemical experiments performed with mutant mouse strains revealed that p23 and p24 are required in the embryonic development in mouse embryos and placenta (Denzel et al., 2000; Jerome-Majewska et al., 2010). In yeast, deletion of the p24 family members shows only a reduction of the transport rate of some cargo and does not affect cell viability or result in a severe protein transport phenotype (Denzel et al., 2000; Marzioch et al., 1999). However, more recently evidence for a direct role of the yeast p24 complex was reported in vesicle budding under coat-limiting conditions (Aguilera-Romero et al., 2008).

Various family members localize within the early secretory pathway (Emery et al., 2000). At a steady state, p24 family members are found abundantly in the CGN (*cis*-Golgi Network)(Dominguez et al., 1998). Biochemical assays and subcellular fractionations revealed that p24 family members are present in different oligomeric states in different organelles. Furthermore, temperature blocks and quantitative western blot analysis in HeLa cells revealed that p24 and p25 localize equally to all membranes. p23 and p27 however, build up opposing gradients, with p23 being more abundant in the ER and ERGIC and less abundant in the Golgi, and p27 showing the opposite gradient (Jenne et al., 2002). While all the other p24 family members occur as dimeric and even tetrameric forms, p26 is present in the early secretory membranes as a monomer, and does not interact with other members of the family (Jenne et al., 2002).

p23 and p24 carry different localization signals in their cytoplasmic tail (Dominguez et al., 1998). The tail of many p24 family members contains phenylalanine residues, whereas only a subset of family members contains a double lysine motif close to the C-terminus (Fiedler et al., 1996; Nickel et al., 1997; Sohn et al., 1996), similar to the cytoplasmic tails of ER resident proteins that contain KKXX retrieval motifs (Nickel et al., 1997). Combination of dilysine and double phenylalanine motifs (FFXX(K/R)(K/R)X_n ($n \geq 2$)) in the cytoplasmic tail of the p24 family members allow the binding to COPI via γ-COP and COPII via Sec23 (Bethune et al., 2006; Dominguez et al., 1998; Nickel et al., 1997; Popoff et al., 2011a). *In vivo* mutational analyses confirm the role of both motifs; mutations in one protein can also effect the location of other non-mutated members of the p24 family, presumable as a consequence of their oligomeric properties (Dominguez et al., 1998).

As different signals keep p24 family members in the early secretory pathway, this could also be the reason for their different kinetics of cycling (Popoff et al., 2011). Immunofluorescence labeling revealed two distinct groups of p24 family members, distinguished by different Golgi to ER travel rates (Eva Emig, PhD thesis). In the light of this preliminary data, we investigated the kinetics of the

p24 family members in more detail. The possibility to categorize the p24 family into two kinetically different subfamilies could help to understand the different functions and/or different trafficking routes within the early secretory pathway of the family members in a more general way. Fluorescent Loss in Photobleaching (FLIP) was used to investigate the export rate of the p24 family members from ER to Golgi (see Chapter IV). Another method to selectively follow up protein trajectories was opened up by the recent development of photoactivatable fluorescent proteins (PAFPs). The PAFP Dronpa is most suitable for our purposes as it is monomeric, brighter than GFP and can be switched on and off by different wavelengths of light more than 100 times (Day and Davidson, 2009). Dronpa tagged p24 protein family members can be activated at the location of interest and their path can be followed up throughout the cell (see Chapter IV).

1.1.2.3. Coatomer

Coatomer is a cytosolic protein complex (550kD), which consist of seven subunits: α-COP (138 kDa), β-COP (107 kDa), β'-COP (102 kDa), γ-COP (97 kDa), δ-COP (57 kDa), ε-COP (34 kDa) and ζ-COP (20 kDa) (Serafini et al., 1991a; Stenbeck et al., 1993; Waters et al., 1991). In an Arf1-GTP dependent manner, the heptameric coat complex is recruited *en bloc* from the cytosol to the membrane (Hara-Kuge et al., 1994).

The two coatomer subunits γ-COP and ζ-COP exist in two homologs termed γ1-, γ2-, and ζ1-, ζ2-COP (Futatsumori et al., 2000). Different homologs of the subunits result in four different isoforms of coatomer. These isoforms are named according to their content of the variable subunits: γ1ζ1, γ2ζ1, γ1ζ2, and γ2ζ2. In mammalian cells, different amounts of these subunits were observed: 53% of γ1ζ1, 26% of γ2ζ1, 16% of γ1ζ2 and 5% of γ2ζ2 isoform (Moelleken et al., 2007). Furthermore, the coatomer isoforms localize at significantly different ratios across the Golgi apparatus of mammalian cells (Moelleken et al., 2007). While γ1ζ1 and γ1ζ2 isoforms were located at the *cis* part of the Golgi, γ2ζ1 isoform was located mainly to the *trans*-Golgi (Moelleken et al., 2007). Different localization and ratios of the coatomer subunits suggests different sites of

budding for each of them with possibly carrying different cargo (Moelleken et al., 2007; Popoff et al., 2011b)

1.2. Unconventional secretion

Unconventional protein secretion summarizes different types of pathways, which are independent of the conventional secretory pathway (ER-Golgi). Unconventionally secreted proteins lack signal peptides, and either bypass an organelle of the conventional pathway or do not enter at all (Nickel, 2010; Rabouille et al., 2012). These proteins are not affected by inhibitors of vesicular transport like e. g. Brefeldin A (Nickel, 2010). An increasing number of proteins are found to be secreted unconventionally, e.g. SH4 domain containing proteins. Parasitic surface protein HASPB (hydrophilic acylated surface protein B) and Src kinase Yes both are examples of N-terminal SH4 domain containing proteins (Tournaviti et al., 2007). The SH4 domain is required and sufficient for proper transport and attachment of HASPB and Yes to the plasma membrane (Ritzerfeld et al., 2011).

Data based on a genome-wide screen suggests that down regulation of certain coatomer subunits disturbs secretion of some SH4 domain containing reporter proteins (SH4-proteins). Furthermore, after knockdown of γ2-COP (but not γ1-COP) the SH4 domain containing protein HASPB accumulates in the perinuclear region, while Yes is correctly transported to the plasma membrane (Walter Nickel, unpublished). In the light of this information, we investigated the possible function of the γ2-COP in the transport of the SH4 proteins. To this end, stable cell lines expressing the SH4-proteins were used to perform coatomer subunit knockdowns for investigating intracellular localization of the reporter proteins under the knockdown conditions (Ritzerfeld et al., 2011)(see Chapter I).

2. Materials and Methods

2.1. Materials

2.1.1. Chemicals and Consumables

Instead of the once which are mentioned specifically, commonly used chemicals and consumables were purchased from the listed companies below. Merck (Darmstadt), Sigma (Deisenhofen), Roth (Karlsruhe), Fluka (Taufkirchen), Qiagen (Hilden), BioRad (Munich), Boehringer (Mannheim) and Life Technologies (Darmstadt).

2.1.2. Enzymes

EcoRI	New England Biolabs (Frankfurt am Main, Germany)
BamHI	New England Biolabs (Frankfurt am Main, Germany)
BamHI Hi-Fi	New England Biolabs (Frankfurt am Main, Germany)
NotI	New England Biolabs (Frankfurt am Main, Germany)
XbaI	New England Biolabs (Frankfurt am Main, Germany)
XhoI	New England Biolabs (Frankfurt am Main, Germany)
SbfI	New England Biolabs (Frankfurt am Main, Germany)
SacI	New England Biolabs (Frankfurt am Main, Germany)
SacII	New England Biolabs (Frankfurt am Main, Germany)
FspI	New England Biolabs (Frankfurt am Main, Germany)
PvuI	New England Biolabs (Frankfurt am Main, Germany)
DpnI	New England Biolabs (Frankfurt am Main, Germany)
Taq Polymerase	Bio-cat (Heidelberg, Germany)
Pfu Turbo Polymerase	Agilent Technologies(Germany)
Taq Polymerase	Axon Labortechnik (Germany)
T4 DNA Ligase	Thermo Scientific (Germany)

2.1.3. Antibodies

2.1.3.1. Primary Antibodies

Epitope	Name	Species	Dilution (WB)	Dilution (IF)
p23	Henriette	Rabbit	1:10 000	-
p24	Elfriede	Rabbit	1:10 000	-
TMED2	TMED2	Mouse	1:1000	-
α-COP	1PSL	Rabbit	1:1000	-
β-COP	B1, 2	Rabbit	1:2000	-
δ-COP	R877	Rabbit	1:1000	-
γ1-COP	g1.2	Guinea pig	1:10 000	-
γ2-COP	g2.2	Guinea pig	1:10 000	-

Epitope	Name	Species	Dilution (WB)	Dilution (IF)
γ1/γ2-COP	γ-r	Rabbit	1:10 000	-
ζ1-COP	R468.1	Rabbit	1:5000	-
ζ2-COP	R442	Rabbit	1:5000	-
GAPDH	GAPDH	Mouse	1:5000	-
GFP	Abcam	Mouse	1:1000	-
GFP	Abcam	Goat	used for IP	used for IP
GFP	Abcam	Rabbit	1:1000	-
Tubulin	YL1/2	Rat	1:500	-
MannosidaseII	Rab1	Rabbit	1:1000	-
MannosidaseII	Rab2	Rabbit	-	1:100-1:500
GM130	GM130	Mouse	-	1:1000
Calnexin	Stressgen	Rabbit	-	1:100
Lamp2	Lamp2	Rat	-	1:100
EEA1	EEA1	Goat	-	1:100
ERGIC53	ERGIC53	Mouse	-	1:100
KDEL	KDEL	Mouse	-	1:100

TABLE 1: List of primary antibodies used

2.1.3.2. Secondary Antibodies

2.1.3.2.1. Antibodies for Immunofluorescence Labeling

Alexa Fluor® 488 Goat Anti-Rabbit IgG (H+L)
Alexa Fluor® 488 Goat Anti-Mouse IgG (H+L)
Alexa Fluor® 546 Goat Anti-Rabbit IgG (H+L)
Alexa Fluor® 546 Goat Anti-Mouse IgG (H+L)

2.1.3.2.2. Antibodies for Li-COR Odyssey

Alexa Fluor 680 goat anti-rabbit IgG
Alexa Fluor 680 goat anti-mouse IgG

Secondary antibodies were manufactured by Life Technologies (Darmstadt, Germany).

2.1.4. Bacterial Strains

The *E. coli* strains DH5α and DH10ß; used for subcloning and plasmid propagation were purchased (Invitrogen, Carlsbad, USA).

2.1.5. Protease Inhibitors

To inhibit the protease activity in the cell lysis protocols Protease-inhibitor-cocktail tablets (Complete, EDTA-free) manufactured by Roche (Mannheim, Germany) were used.

2.1.6. Protein and DNA Standards

Precision Plus Protein™ All Blue Standards	Bio-Rad Laboratories GmbH (Munich, Germany)
100 bp DNA Ladder	New England Biolabs (Frankfurt am Main, Germany)

2.1.7. Chemical Crosslinkers

DMP (Dimethyl pimelimidate•2 HCl)	Thermo Scientific (Illinois, USA)
DSG (Disuccinimidyl glutarate)	Thermo Scientific (Illinois, USA)

2.1.8. Transfection Reagents

Oligofectamine™ Transfection Reagent	Life technologies (Darmstadt, Germany)
Lipofectamine™ 2000 Transfection Reagent	Life technologies (Darmstadt, Germany)
FuGENE® HD Transfection Reagent	Promega (Wisconsin, USA)

2.1.9. MRA Treatment

Mycoplasma Removal Agent	MP Biomedicals (California, USA)

2.1.10. Antibiotics

Doxycycline	BD Biosciences (California, USA)
Ampicilin	GERBU Biotechnik GmbH (Heidelberg, Germany)
Kanamycin	GERBU Biotechnik GmbH (Heidelberg, Germany)

2.1.11. Growth Media

LB (Luria Broth) Media was used to grow the *E.coli* strains.

2.1.12. Cell Lines

Name of the Cell Line	Cell Line	Origin	Medium	Creator
3T3	3T3/NIH MCAT	Mouse fibroblast	DMEM + all (FCS)	ATCC
HA-g1 (18 KlonXII)	3T3/NIH MCAT	Mouse fibroblast	DMEM + all (FCS)	Jörg Moelleken
Myc-g2 (24 Klon A41)	3T3/NIH MCAT	Mouse fibroblast	DMEM + all (FCS)	Jörg Moelleken
HeLa-double5 (SH4-HASPB-GFP/SH4-Yes-Cherry#5)	HeLa	Human Cervical Cancer	DMEM + all (FBS)	Julia Ritzerfeld
HeLa-MCAT	HeLa	Human Cervical Cancer	DMEM + all (FBS)	Nickel Lab.
HeLa-mcat-YFP-p24	HeLa	Human Cervical Cancer	DMEM + all (FBS)	Andreas Max Ernst
HeLa-mcat-YFP p24 (TMD)L17	HeLa	Human Cervical Cancer	DMEM + all (FBS)	Andreas Max Ernst
HeLa Paris	HeLa	Human Cervical Cancer	DMEM + all (FBS)	Institute Curie
HeLa DSMZ	HeLa	Human Cervical Cancer	DMEM + all (FBS)	DSMZ
HEK293T	HEK293T	Human embryonic kidney	DMEM + all (FBS)	ATCC
CHO	CHO	Chinese Hamster Ovary	DMEM + all (FBS)	ATCC
C3-14	CHO	Chinese Hamster Ovary	DMEM + all (FBS)	Christoph Rutz
C3-30	CHO	Chinese Hamster Ovary	DMEM + all (FBS)	Christoph Rutz
C4-53	CHO	Chinese Hamster Ovary	DMEM + all (FBS)	Christoph Rutz
Y3-9	CHO	Chinese Hamster Ovary	DMEM + all (FBS)	Christoph Rutz
Y4-9	CHO	Chinese Hamster Ovary	DMEM + all (FBS)	Christoph Rutz

TABLE 2: List of cell lines used

2.1.13. Molecular Biological and Biochemical Kits

MBS Mammalian Transfection Kit	Stratagene (La Jolla, USA)
Mycoplasma PCR Elisa Kit	Roche (Grenzach-Wyhlen, Germany)
NucleoSpin Plasmid	Macherey-Nagel (Düren, Germany)
QIAprep SPIN Miniprep Kit	Qiagen GmbH (Hilden, Germany)
QIAgen Plasmid Maxi Kit	Qiagen GmbH (Hilden, Germany)

QIAquick Gel Extraction Kit	Qiagen GmbH (Hilden, Germany)
QIAquick PCR Purification Kit	Qiagen GmbH (Hilden, Germany)
Bio-Rad Protein Assay	Bio-Rad Laboratories GmbH (Munich, Germany)
BCA Protein Assay	Thermo Scientific Pierce (Illinois, USA)
RNeasy Mini Kit	Qiagen GmbH (Hilden, Germany)
The ImProm-II Reverse Transcription System	Promega (*Wisconsin*, USA)

2.1.14. Cell Culture Medium and Supplements

Opti-MEM® I Reduced Serum Media	Life technologies (Darmstadt, Germany)
Dulbecco's Modified Eagle Medium (DMEM)	Biochrom (Berlin, Germany)
L-Glutamine	Biochrom (Berlin, Germany)
Fetal Calf Serum	PAA Laboratories GmbH (Cölbe, Germany)
Fetal Bovine Serum	PAA Laboratories GmbH (Cölbe, Germany)
Penicilin/Streptomycin	Biochrom (Berlin, Germany)

2.1.15. List of siRNA's

Subunit	**Ambion ID**	**siRNA name**	**Stock Concentration**
gamma1-COP	237500	115	30μM
gamma1-COP	237501	116	30μM
gamma1-COP	-	Silencer select	30μM
gamma2-COP	s25643	Gamma2	30μM
zeta1-COP	s22427	Zeta1	30μM
zeta2-COP	s27712	Zeta2	30μM
alpha-COP	146404	Alpha	30μM
delta-COP	10234	Delta	50μM
beta-COP	s3371	Beta	50μM
GFP	AM4626	GFP	50μM
Scrambled siRNA	-	Scrambled siRNA	50μM
Qiagen all-star negative control	Qiagen	All-star negative control	50μM
Subunit	**Dharmacon ID**	**Lot #**	**Stock Concentration**
gamma1-COP	L-019138-00	100301	50μM
gamma2-COP	L-019988-01	100301	50μM
zeta2-COP	L-021116-01	100301	50μM
p24-TMED2	J-008074-09	-	20μM

TABLE 3: List of siRNA's used

2.1.16. List of Primers

PFB	
Forward	5'-CGA ACC CCA GAG TCC CGC TCA-3'
Forward new	5'-TGG AGA CTA AAT AAA ATC TT-3'
Reverse	5'- GGC TGC CGA CCC CGG GGG TGC-3'
FGF4	
Forward	5'-TTG GAT CCG CCA CCA TGG-3'
Reverse	5'-TTG CGG CCG CTT ACT TGT ACA GCT CGT CCA TG-3'
AgeI@599mut	
Forward	5'-CGC TAG CGC TAG CGG TCG CCA CCA TG-3'
Reverse	5'-CAT GGT GGC GAC CGC TAG CGC TAG CG-3'
DRONPA-AgeI	
Forward	5'-ATA TCT ACC GGT AAT GGT GAG TGT GAT TAA ACC-3'
Reverse	5'-GAT ATG AAT TCA GCT TGG CCT GCC TCG GCA GCT CAG -3'
HindIII(BamHI)-p23	
Reverse	5'-GCC GCA AGC TTT TAC TCT ATC AAC TTC -3'
NotI(BamHI)-p23	
Reverse	5'-GCC GCG CGG CCG CTT ACT CTA TCA ACT TC-3'
EcoRI-linker2	
Forward	5'-AAT TCA TCC GGA CTC AGS TCT CGA GCT CAA GCT TCG -3'
Reverse	5'-AAT TCC GAA GCT TGA GCT CGGA GAT CTG AGT CCG GAT G-3'

2.1.17. Software's

ZEN 2009 and 2010	Carl Zeiss Jena GmbH (Jena, Germany)
Fiji 1.46j	ImageJ (NIH, USA)
Volocity 5.2.1	Perkin Elmer (Massachusetts, USA)
Graphpad Prism 5	GraphPad Software, Inc. (California, USA)
DNA Strider 1.4f6	CEA (France)
4Peaks,Version 1.7.2 (1.7.1)	Mek&Tosj (Amsterdam, The Netherlands)
Image Studio	LI-COR Biosciences GmbH (Bad Homburg, Germany)

2.1.18. Technical Devices

Instead of the once which are mentioned specifically, commonly used chemicals and consumables were purchased from the listed companies below. Infors AG (Einsbach), Braun (Melsungen), Eppendorf (Hamburg), Kendro (Langenselbold), Zeiss (Göttingen), Becton Dickinson (Heidelberg), PerkinElmer (Massachusetts, USA), Bio-Rad Laboratories GmbH (München), Peqlab (Erlangen), Gilson (Villiers-le-Bel,France), NeoLab (Mannheim).

2.1.19. Buffers

PBS (10X)
1,37 M NaCl
43 mM $Na_2HPO_4x2H_2O$
27 mM KCl
15 mM KH_2PO_4
$\Rightarrow$ pH = 7.4

PBS-T
1X PBS
0,05% (v/v) Tween-20
$\Rightarrow$ pH = 7.4

Lysis Buffer I (for siRNA knockdown experiments)
1X PBS
1% (w/v) TritonX100
Protease Inhibitor Cocktail tablet (freshly added)

Lysis Buffer II
20 mM HEPES
100 mM NaCl
5 mM EDTA
0.5% Sodium Deoxycholate
1% TritonX100
$\Rightarrow$ pH 7.4
Protease Inhibitor Cocktail tablet (freshly added)

Lysing Buffer III (containing 4% octylglucoside)
20 mM HEPES
50 mM NaCl
4% Octylglucisidase (n-octyl-β-D-glucoside)
$\Rightarrow$ pH 6.8

PBS/EDTA
1:1000 EDTA (stock concentration: 0.5 M pH 7.8) in PBS

5X DNA Loading Buffer
0.25% (w/v) Bromophenol blue
30% (w/v) Glycerol
10 mM Tris-HCl pH 8.0

50X TAE
40 mM Tris-HCl
20 mM Acetic Acid
1 mM EDTA
⇒ pH 8.0

4X SDS Loading Buffer
200 mM Tris-HCl pH 6.8
40 % (v/v) Glycerol
12 % (v/v) β-mercaptoethanol
8 % (w/v) SDS
0.2 % (w/v) Bromophenol Blue

SDS-page Running Buffer
25 mM Tris
192 mM Glycine
0.1% (w/v) SDS

Blotting Buffer
25 mM Tris
250 mM Glycine
20 % (v/v) Methanol

IP Buffer I
20 mM HEPES-KOH
50 mM NaCl
4% (w/v) Octyl glucoside (*n*-octyl-β-D-glucoside)
⇒ pH 6.8

IP Buffer II
25 mM Tris-HCl
150 mM NaCl
1 mM EDTA
⇒ pH 7.4

Cultivation Medium (DMEM+all)
10% (v/v) FBS
2 mM L-Glutamate
100 units/ml Penicillin
100 µg/ml Streptomycin

Freezing Medium
40% FBS
10% DMSO

in DMEM + all

Sorting Medium
5% Cell Dissociation Buffer
0.2% FBS
2 mM L- Glutamate
100 units/ml Penicillin
100 µg/ml Streptomycin
in DMEM

2.2. Methods

2.2.1. Molecular Biological Methods

2.2.1.1. Polymerase Chain Reaction (PCR)

PCR Reaction I

100 ng	DNA template
1 µl	Forward Primer (10 pmol/µl)
1 µl	Reverse Primer (10 pmol/µl)
1 µl	dNTP's (10 mM each)
5 µl	10X Pfu Buffer
1 µl	Pfu Turbo Polymerase (2.5 u/µl)
Up to 50 µl	H_2O

PCR Reaction II

100 ng	DNA template
1 µl	Forward Primer (10 pmol/µl)
1 µl	Reverse Primer (10 pmol/µl)
1 µl	dNTP's (10 mM each)
5 µl	$MgCl_2$ (25mM)
5 µl	10X Buffer
1 µl	Taq Polymerase
Up to 50 µl	H_2O

According to the polymarease, which was chosen, one of the two standard PCR reactions above were used to amplify or introduce a particular piece of DNA sequence.

PCR program

Start	98°C	5 min	
Denaturation	98°C	30 sec	} Amplification (30 cycles)
Hybridization	60°C	30 sec	
Elongation	72°C	1 min/kb target gene	
End	72°C	5 min	
Store	4°C	∞	

2.2.1.2. PCR Purification

Using QIAquick PCR Purification Kit the PCR products were purified and DNA was eluted in 50 µl H_2O.

2.2.1.3. Site-Directed Mutagenesis

Site-directed mutagenesis was used to do point mutations in the gene of interest.

PCR Reaction

100 ng	DNA template
1 µl	Forward Primer (100 pmol/µl)
1 µl	Reverse Primer (100 pmol/µl)
1 µl	dNTP's (10 mM each)
5 µl	10X Pfu Buffer
1 µl	Pfu Turbo Polymerase (2.5 u/µl)
Up to 50 µl	H_2O

PCR Program

Start	98°C	2 min	
Denaturation	98°C	30 sec	} Amplification (18 cycles)
Hybridization	50°C	1 min	
Elongation	68°C	10 min	
End	68°C	15 min	
Store	4°C	∞	

After the polymerase chain reaction DpnI treatment followed for 2 h at 37°C. 2 µl DpnI enzyme was added to each reaction.

2.2.1.4. Restriction Digest

Standard Reaction (total volume 50 µl)

DNA	1 µg
Restriction Enzyme	1 µl (10 U)
10X NEBuffer	5 µl (1X)
BSA (if necessary)	add to a final concentration of 100 µg/ml (1X)
H_2O	up to 50 µl

In a common reaction the incubation time is 1 h and the temperature is 37°C. Depending on the enzyme(s) used for the restriction endonuclease digest, incubation time and incubation temperature were defined.

2.2.1.5. Ligation of DNA Fragments

Ligation of DNA fragments were performed by catalyzing the formation of the phosphodiester bonds between the strands with the enzyme called T4 DNA ligase. Ligation reaction was set according to the Ligation Equation below and incubated for either 1h at room temperature or overnight at 4°C.

Ligation Equation

Insert Size (bp)/Vector Size (bp) X Vector Amount (µg) X 5 = Insert Amount (µg)

2.2.1.6. Heat Shock Transformation of Competent Bacteria

100 µl of DHα5 *E.coli* competent cells were mixed with 2-5 µl ligation reactions and incubated on ice for 30 min. Heat shock is performed for 90 sec at 42°. Immediately after the heat shock, cells are places on ice for 10 min and 900 µl LB medium was added on the cells. Cells were incubated at 37°C with agitation for 1 h and centrifuged for 1 min at 13.000 rpm. Afterwards 900 µl of the medium is discarded. Sedimented cells were resuspended with remaining medium and plated on an agar plate containing appropriate antibiotic and allowing the colonies to grow overnight at 37°C.

2.2.1.7. Plasmid Preparation from Bacteria

The method was used to extract and purify DNA of interest from *E.coli*. Growth

of the bacteria was allowed in LB medium supplemented with antibiotics (Ampicilin or Kanamycin) according to the plasmid selection marker. Plasmid DNA was extracted and purified using Qiagen Kits according to manufacturer's instructions. DNA was eluted in desired amount of H_2O and DNA concentration was determined by NanoDrop ND-1000 spectrophotometer.

2.2.1.8. Agarose Gel Electrophoresis

Agarose gel electrophoresis was used to separate the DNA fragments. 1% agarose gel was prepared by solving the 0.5 g Agarose NEEO Ultra-Qualität (Roth, Germany) in 50 ml 1X TAE buffer. After cooling down, Ethidium Bromide was added for detection of DNA to final concentration of 0.5 µg/ml. Gel was poured into gel cast for solidification and combs were inserted to create wells for loading samples.

Samples were mixed with 5X DNA Loading Buffer and loaded in the wells of the 1% agarose gel. In addition to the samples, 1 kb DNA Ladder was loaded on a gel as a reference of size of the DNA fragments. Electrophoresis was performed in 1X TAE Buffer with 100 V to separate the samples in PeqLab Gel Chamber. DNA bands were visualized in BioRad Gel Doc 2000 under 260 nm UV light.

2.2.1.9. Gel Extraction

DNA containing bands of the 1% agarose gel were cut. DNA was extracted by using Qiagen Gel Extraction Kit according to manufacturer's instructions.

2.2.1.10. DNA Sequencing

The prepared DNA sent to the company called GATC Biotech AG (Konstanz, Germany) for determining the order of nucleotides. DNA sequences sent by the company were compared to theoretical sequences by DNA Strider and 4Peaks software's.

2.2.1.11. Alcohol precipitation

Precipitation of the DNA was done by adding 3 M sodium acetate pH 5.0, 1:10 volume of the DNA and 2.5X 100% EtOH. DNA was incubated at -20°C for 20 min. Centrifugation followed for 15 min at 13.000 rpm. The pellet was washed with 70% EtOH and spun down again at 13.000 rpm only for 5 min. And the pelleted DNA was resuspended with H_2O.

2.2.1.12. Glycerol stock preparation

After the heat shock transformation the bacteria containing desired plasmids were stored in glycerol stocks. 800 µl of inoculated bacteria in LB medium with 200 µl of autoclaved 80% Glycerol were mixed immediately and snapped freeze in liquid nitrogen. Stored at -80°C.

2.2.1.13. Determination of DNA-concentration

DNA concentration was determined by NanoDrop ND-1000 spectrophotometer. 1-2 µl DNA was measured with 260 nm wavelength.

2.2.1.14. Cell Culture Techniques

2.2.1.14.1. Maintenance of the Adherent Cells

Adherent cells were cultivated in petri dishes of various sizes in an appropriate medium at 37°C with 5% CO_2. When the cells reached to 95-100% confluency the cells were passaged to continue normal growth. For passaging the cells, the growth medium was discarded. Cells were rinsed with PBS and dissociated from the petri dishes by adding ~1 ml Tyripsin/EDTA (for 10 cm petri dish) and incubating at 37°C for 3-5 min. Fresh medium added onto tyripsinized cells and plated on desired amount of cell to a new petri dishes. The cells were incubated in 37°C with 5% CO_2 for normal growth.

2.2.1.14.2. Freezing cells

Cells were grown in 10 cm petri dishes until the 80-90% confluency. Rinsed and tyripsinized as explained above. 10 ml fresh medium is added and the cells were collected in 15 ml conical tube. Centrifugated cells for 3-5 min at 1000 rpm were pelleted. Tyripsin containing medium was discarded and the pellet was resuspended with 1.5 ml freezing medium. Cells were placed into cryo vials and stored at -80°C. For long-term storage cryo vials were placed into liquid nitrogen tanks.

2.2.1.14.3. Thawing cells

Frozen cells in the cryo vials were immediately placed in 37°C water bath for fast thawing. Cells were transferred to a 50 ml conical tube containing pre-warmed 20 ml growth medium. Cells were centrifuged for 5 min at 1000 rpm and the medium was discarded. Pelleted cells were gently mixed with fresh medium and plated in a petri dish. Cells were incubated at 37°C with 5% CO_2 for normal growth.

2.2.1.14.4. Transient Transfection of Mammalian Cells

Method was used for expressing exogenous DNA in mammalian cells. Cells were plated into petri dishes or 6-well plates in 60-70% confluency 24 h prior to the transfection. Lipofectamine or Fugene were used to transiently transfect plasmid DNA to mammalian cells according to manufacturer's instructions.

2.2.1.14.5. Retroviral Transduction of Mammalian Cell Lines

Generating stable cell lines was performed by retroviral transfections. For retroviral transfection of the mammalian cell lines, the MBS Mammalian Transfection Kit (Stratagene) was used according to manufacturer's instructions. Plasmid containing retroviral particles were produced in HEK293T cell lines with help of two vectors (pVPack-GP and pVPack-Eco) and the plasmid. Supernatant containing viral particles was used for transduction of the HeLa-MCAT cell lines. 48-72 h after transduction the cells were sorted for

Doxycycline inducible reporter gene expression from the pRev-TRE2 vector by several rounds of FACSAria flow cytometer sorting.

2.2.1.14.6. Fluorescence-Activated Cell Sorting (FACS)

FACS sorting was used to select the cells stably expressing the reporter proteins in a doxycycline inducible manner. Cells were plated 48 h prior to the sorting and 24 h before the sorting 1 µg/ml doxycycline was added or not (for “bright” or “dark” sorting, respectively). Cells were washed with PBS and detached from the dish using Cell Dissociation Buffer. Cells were collected with Sorting Medium and passed through a cell strainer cap (Becton Dickinson). FACSAria flow cytometer was used sort the cells according to the expression of the reporter proteins fluorescence characteristics. To collect a pool of cells which expresses the reporter protein in a tightly doxycycline inducible manner, the cells were subjected to subsequent three sorting, namely, bright, dark and bright sort. First sorting was for the fluorescent cells, which was induced with doxycycline. Second sort were uninduced cells, which don’t expressed the reporter protein. This sort was for separating the leaky cells expressing the reporter protein in the absence of doxycycline. And the final sort was bright sort with induced cells lead to a pool of doxycycline-induced cells.

2.2.1.14.7. siRNA Transfection of Mammalian Cells

Adherent HeLa cells were siRNA transfected using Oligofectamine transfection reagent in 6-well plates. Cells were plated on 6-well plates 24 h prior to the transfection in 60% confluency. Following day, 50 pmol siRNA (30-50 µM) was diluted in 180 µl Opti-MEM and mixed with 48 µl Oligofectamine diluted 1:4 in Opti-MEM (12 µl Oligofectamine, 36 µl Opti-MEM). This siRNA and oligofectamine mixture was incubated for 20 min at room temperature. While this mixture was incubated, cells were washed with oligofectamine and 1.5 ml fresh oligofectamine were added in each well. Afterwards, siRNA-Oligofectamine mixture is slowly added to each well while gently mixing the plate. Cells were incubated for 4 to 6 hours at 37°C and medium was exchanged with a normal growth medium. 24 h after transfection cells were split

to suitable dishes for microscopy, in addition to fresh 6-well plates. In the case of doxycycline induction, cells were incubated the last 24 h in the presence of 1 µl/ml doxycycline at 37°C.

2.2.1.15. Fluorescence Microscopy Techniques

2.2.1.15.1. Wide-field and Confocal Microscopy

Imaging of the cells was performed with wide-field or confocal microscopes. Live cell imaging is performed with imaging medium containing HEPES and fixed cells were subjected to immunofluorescence staining. Axiovert 200M fluorescence microscope (Zeiss), LSM 510 confocal microscope (Zeiss), LSM 780 confocal microscope and Perkin–Elmer Ultra-view spinning disk confocal microscope were used for imaging.

2.2.1.15.2. Immunofluorescence Labeling

Cells were plated on a Mattek dishes or cover slips for microscopy. Cells were fixed with 4% paraformaldehyde for 20 min following the quenching with 50 mM ammonium chloride for 15 min cells were blocked with 5% BSA for 15 min. After that cells were subjected to primary and secondary antibodies subsequently for 30 min at room temperature. Between all the steps cells were rinsed with 1X PBS. Cover slips were mounted with DAPI containing The ProLong® Gold Antifade Reagent (Life Technologies).

2.2.2. Biochemical Methods

2.2.2.1. Cell Lysis for siRNA Knockdown Experiment

Cells were placed on ice and rinsed with chilled 1X PBS. 500 µl PBS/EDTA added on and the cells were scraped. Collected cells in eppendorf tubes were centrifuged at 200 g for 3 min at 4°C. The pellet was resuspended in 80 µl PBS/TritonX100/Protease Inhibitor Cocktail and lysed by vortexing every 10 min for 30 min. Afterwards cells were agitated with sonification for 5 min and centrifuged at 14.000 rpm for 15 min at 4°C. Supernatant was subjected to BCA protein determination. During the whole procedure the cells were kept on ice.

2.2.2.2. Cell Lysis

Cells were placed on ice and rinsed with chilled PBS. For 10 cm petri dishes 800 µl PBS added to the cells and cells were scraped. Collected cells were centrifuged at 6500 rpm for 5 min at 4°C. The pellet was resuspended with 100 µl Lysis Buffer II and agitated on overhead rotator at 4°C for an hour. Cells were centrifuged at 6500 rpm for 5 min at 4°C. Lysate was subjected either to SDS-page analysis or immune precipitation.

2.2.2.3. Protein Concentration Determination

Two different methods were used to determined protein concentrations in the cell lysates or tissue samples namely; Bradford and BCA assays. For Bradford assay Bio-Rad Kit from Bio-Rad and for BCA assay BCA Protein Assay Kit from Thermo Scientific Pierce were used according to manufacturer's instructions.

2.2.2.4. *In vivo* Crosslinking

DSG (Disuccinimidyl glutarate) was used for *in vivo* crosslink experiments with stable cell lines expressing protein of interest in Doxycycline inducible manner. 30.10^4 cells/well plated in a 6-well plate and incubated for 24 h with 1 µg/ml doxycycline. Cells were washed with PBS and incubated with the permeable cross-linker DSG (0.5 mM in 5 µl DMSO) in PBS for 15 min at room temperature. After cross-linking, cells were quenched with 100 mM Glycine pH 3 and 500 mM Tris pH 8 subsequently for 15 min each at room temperature. Cells were washed with PBS and lysed as described in "Cell Lysis" previously. The lysate was heated at 65°C for 10 min in sample buffer containing 50 mM DTT (freshly added). Samples were subjected to SDS-PAGE analysis and western blotting.

2.2.2.5. Immune-precipitation

After 24 h incubation with doxycycline the cells were lysed according to "Cell Lysis" protocol described above. Fresh lysate was mixed with 20 µl Protein A beads (which was chosen according to the antibody) and 5 µl anti-GFP

antibody (Abcam) and incubated overnight at 4°C on an overhead rotator. The beads were washed for five times with 1 ml Lysis Buffer II and then eluted in 30 µl sample buffer by boiling for 5 min at 95°C. Finally, the samples were analyzed with SDS-PAGE and western blot.

2.2.2.6. SDS-Page (Sodium Dodecyl Sulfate Polyacrylamide Gel Electrophoresis) Analysis

Proteins were separated according to their electrophoretic mobility. Lysed cells or tissue samples were SDS treated and run in defined gel compositions.
Gels are consists of two different layers: Stacking gel and separating gel. Acrylamide concentration of the separating gel defines the gel structure. Also different acrylamide/bisacrylamide ratios can be used for special purposes.

Stacking Gel

Gel concentration	**4%**
0.5 M Tris/HCl (pH 6.8)	2.5 ml
H_2O	6.1 ml
Acrylamide	1.3 ml
10% SDS	100 µl
APS	100 µl
TEMED	10 µl

Separating Gel

Gel concentration	**6%**
1.5 M Tris/HCl (pH 8.8)	3.75 ml
H_2O	8.1 ml
Acrylamide	3 ml
10% SDS	150 µl
APS	150 µl
TEMED	15 µl

Gels were polymerized in between two glass plates in a way the separating gel at the bottom and the stacking gel on top. Using combs, pockets were introduced allowing different samples to be loaded. Samples were diluted in 4X SDS Loading Buffer and boiled at 95°C for 5 min. Polymerized gels were placed in a gel chamber with Running Buffer and the samples were loaded in the wells. Along with the samples protein marker (Precision Plus Protein™ All Blue

Standards) was loaded to use as a standard of molecular weights. Chamber is securely closed and the electric field was applied to the gel, allowing the negatively charged molecules migrate through the gel matrix. Constant 100 V is applied until the front-dye reaches the end of the gel for proper separation of the proteins.

2.2.2.7. Western Blot Analysis

Separated proteins by SDS-Page transferred onto PVDF membranes (Millipore, Schwalbach) via “Wet-Blot” method. Assembly of the system requires filter papers, PVDF membrane, Methanol and Blot Buffer. Filter papers were soaked in blot buffer and the PVDF membrane was soaked first in methanol for activation and then in blot buffer for equilibration. From bottom to top components of the sandwich was placed in cassettes; sponge, two filter papers, polyacrylamide gel, PVDF membrane, again two filter papers and sponge. Closed the cassette carefully and placed it in a chamber. Put an icepack in the chamber to keep it cool and a stir bar for even distribution of the ions and the temperature. Closed the chamber securely and under constant voltage (for 0.75 mm thickness of the gels; 100 V for 1 h or 30 V for overnight) transferred the proteins to the PVDF membrane. The membrane containing proteins was ready to further process.

2.2.2.8. Immune-blot Analysis

Membranes were rinsed with PBS-T briefly and blocked with 5% milk in PBS-T for an hour at room temperature. Afterwards membranes were washed with PBS-T twice for 10 min and then incubated with primary antibodies in 1% BSA in PBS-T for 1 h at room temperature. The membranes were washed three times for 10 min at room temperature and incubated with secondary antibody in 1% BSA in PBS-T for 30 min at room temperature in dark. The membranes washed with PBS-T last three times for 10 min. All incubations in the procedure can be done at 4°C overnight. Detection of the membranes was performed by LICOR Odyssey as the manufacturer’s instructions.

3. Results

Different aspects of vesicular transport in the early secretory pathway were investigated in this study. The classical secreted of cargo starts its journey where it is being synthesized and assembled (ER) and then continues in various transport carriers until it reaches its final destination. Unconventionally secreted proteins do not enter this pathway or skip some compartments along their way to their final destination (Nickel and Rabouille, 2009, Rabouille et al., 2012). In the scope of this thesis, the following questions were addressed: i) Does the γ2-COP subunit play a role in the transport of unconventionally secreted SH4 domain containing proteins (HASPB and YES)?, ii) Do novel analogues of the Arf1-GEF complex inhibitor of Brefeldin A affect the Golgi structure in the same way as BFA?, iii) Is the non-SM18 binding mutant of p24 able to form an oligomeric state *in vivo*?, and iv) Are there differences in the kinetics of cycling within the early secretory pathway of the different members in the p24 family?

3.1. CHAPTER I: Role of γ2-COP in the transport of SH4 domain containing proteins

Genome-wide screens based on RNA interference suggest that the transport of SH4 domain containing proteins to the plasma membrane is dependent on coatomer isoforms (Walter Nickel and Rainer Pepperkok, unpublished). More specifically, knockdown of γ2-COP causes a secretion block of SH4 domain proteins, while a knockdown of γ1-COP does not affect the transport of the SH4 domain proteins (Walter Nickel, unpublished). Based on these findings the association of SH4 domain containing proteins and the coatomer subunits is investigated in this chapter.

Considering the preliminary data (Nickel Laboratory, BZH Heidelberg), stable cell lines were produced to express SH4 domain containing reporter proteins in 3T3 cell lines with an established gamma subunit knockdown system. These cell lines were created to further characterize the role of the γ-COP subunits in

the intracellular localization of the aforementioned reporter proteins HASPB and Yes.

In addition to the generation of the cell lines, siRNA knockdown experiments were performed to investigate the effect of coatomer subunits on the intracellular localization of the reporter proteins.

3.1.1. Generation and characterization of stable cell lines expressing SH4 domain containing proteins

Doxycycline inducible stable 3T3 cell lines, as establish earlier in the Wieland Laboratory, were transduced with HA and myc tagged γ1-COP and γ2-COP (respectively) by retroviral transduction. These cell lines 3T3/rtTA-HA-hγ1 and 3T3/rtTA-Myc-hγ2 will be shortened as 3T3g1 and 3T3g2, respectively in the context of this thesis (Joerg Moelleken, PhD thesis). When the cells were characterized, they were found unexpectedly to cause down regulation of the endogenous proteins while the respective exogenous γ-COP subunits was induced. This resulted in only one of the tagged γ-COP subunits being present in mouse fibroblast cell line 3T3 cells after 48 h induction.

The 3T3g1 and 3T3g2 cell lines were then templates for the generation of new cell lines, constitutively expressing SH4 domain containing reporter proteins (SH4-proteins). The SH4-proteins *Leishmania* protein HASPB (Hydrophilic Acylated Surface Protein B) and human Src kinase Yes were used as reporters. The N-terminal 18 amino acids of HASPB and Yes containing the SH4 domain were fused to GFP and mCherry fluorescent proteins, respectively (Julia Ritzerfeld, PhD thesis), resulting in the constructs: SH4-HASPBN18-GFP and SH4-YesN18-mCherry. The fusion proteins were introduced into the 3T3 cells with a gamma subunit knockdown system by retroviral transduction.

Constructs were created from the retroviral vector pRevTRE2 as described in the methods section. A different retroviral vector was chosen to be able to acquire constitutive expression of the reporter proteins. In addition to these

unconventionally secreted reporter proteins, the conventionally secreted FGF4 fused to GFP protein was employed.

Following retroviral transduction, HEK293T cells were cultivated for 48 h and then subjected to the Fluorescence Activated Cell Sorting (FACS). Cell populations are displayed in dot plots; the X-axis represents Forward Scatter (FSC) and the Y-axis represents relative fluorescent intensity (Figure 1). A threshold was set according to expression levels in the negative control cells, not expressing GFP, and positive control cells only expressing GFP. Only cells with a signal intensity above the threshold 10^2 were selected in a pool, since these cells were expressing the fluorescent-tagged exogenous proteins.

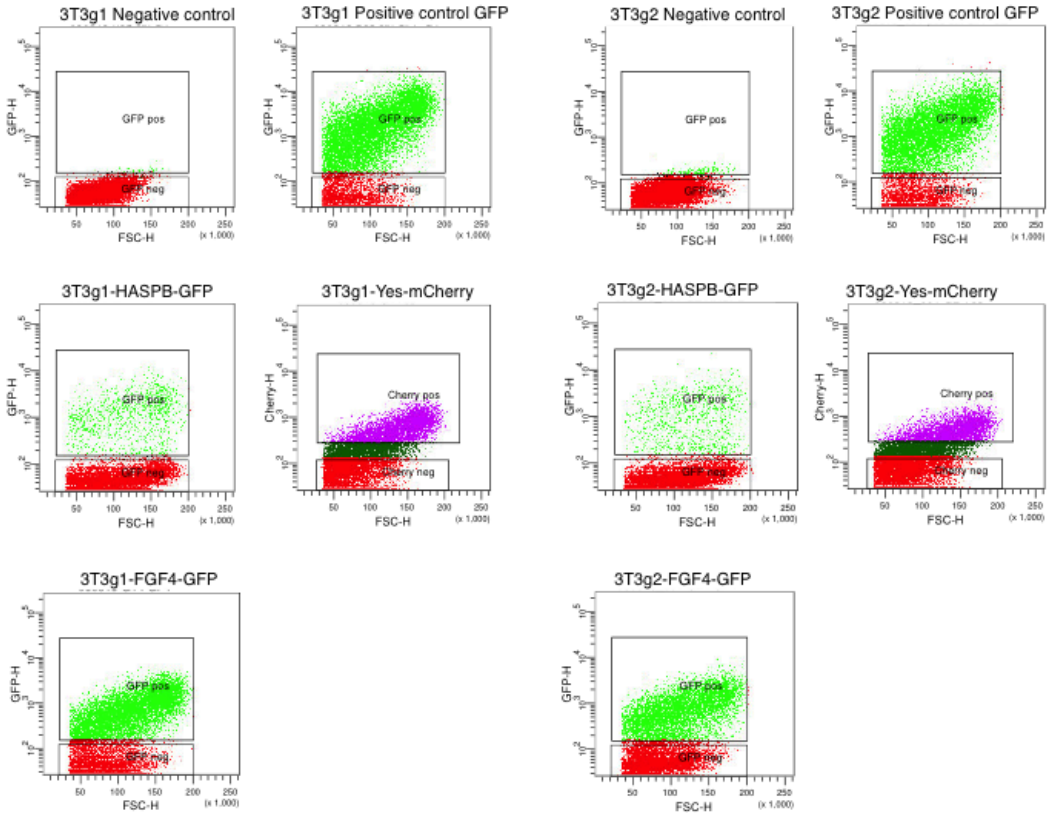

FIGURE 1: Sorting of the stable cell lines by FACS. Stable cell lines expressing the reporter proteins: HASPB, Yes and FGF4, fused to fluorescent tags were generated and sorted by FACS. Non-GFP expressing negative and GFP-only positive control cells were used to set the threshold for the fluorescence intensity. The selected cells were then pooled for further experiments.

Employing the same experimental flow, six different stable cell lines were created and are listed in Table 4.

Name of the Cell Line	Cell line	Origin
3T3g1-FGF4-GFP	3T3/NIH	Mouse fibroblast
3T3g1-SH4-HASPBN18-GFP		
3T3g1-SH4-YesN18-mCherry		
3T3g2-FGF4-GFP		
3T3g2-SH4-HASPBN18-GFP		
3T3g2-SH4-YesN18-mCherry		

TABLE 4: List of Generated Cell Lines.

3.1.2. Characterization of the stable cell lines

Stable cell lines expressing reporter proteins were characterized by fluorescence microscopy and immune-precipitation.

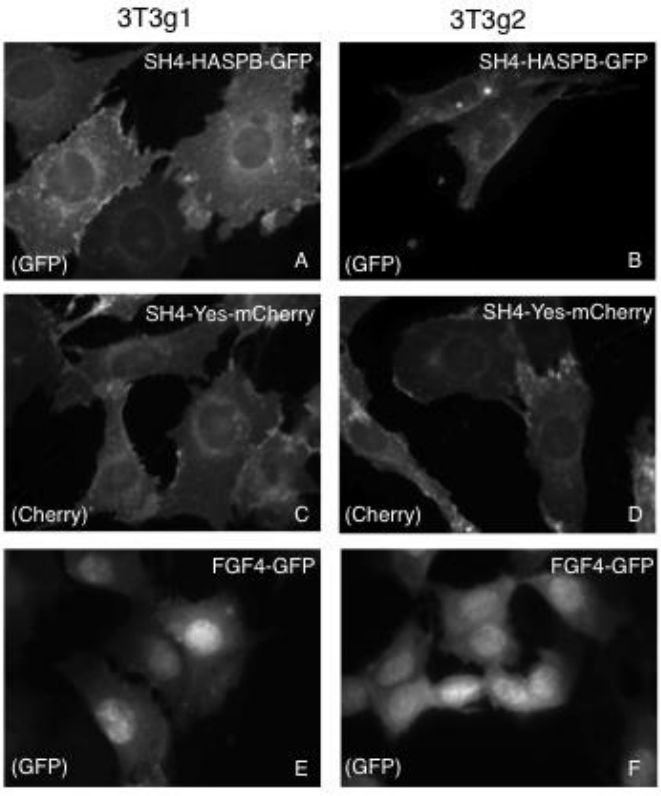

FIGURE 2: Localization of the exogenous SH4-proteins in 3T3g1 and 3T3g2 cell lines. Cell lines expressing HASPB-GFP, Yes-mCherry and FGF4-GFP were induced with doxycycline and visualized by fluorescence microscopy. GFP excitation: 488 nm, Cherry excitation: 560 nm.

When the cells lines were examined with confocal microscopy, homogenous expression of the reporter proteins was observed at low magnification (data not shown). Examination with high magnification, however, showed plasma membrane localization of HASPB-GFP and Yes-mCherry fusion proteins (Figure 2, A-D). FGF4-GFP was localized partially to the nucleus and partially at the cytosol (Figure 2, E-F). FGF4 was not found at the plasma membrane. As FGF4 is known to be secreted into the medium, its concentration in the exocytic pathway was probably too low to be detected.

In summary, in six different stable 3T3 cell lines expressing the SH4-proteins fused to fluorescent reporter proteins were localized at the plasma membrane.

3.1.2.1. Intracellular localization of the SH4-proteins in 3T3 cell lines

Expression of HASPB and Yes was induced under conditions where only one γ-COP subunit was expressed. Cells were treated with doxycycline for 24 h, 48 h and 72 h and the localization of the reporter proteins was visualized by confocal microscopy. Doxycycline induced cells display plasma membrane localization of the reporter proteins HASPB and Yes, and nuclear and cytosolic localization of FGF4, similar to the non-doxycycline treated control cells (data not shown).

3.1.2.2. Monitoring the gamma knockdown system in 3T3 cell lines

Stable cell lines were also analyzed biochemically to examine if the property of template cell lines were altered during generation of the new stable cell lines. In 3T3g1-HASPB-GFP and 3T3g2-HASPB-GFP cell lines γ-COP levels were detected by immune precipitation after doxycycline induction for 24 h, 48 h and 72 h.

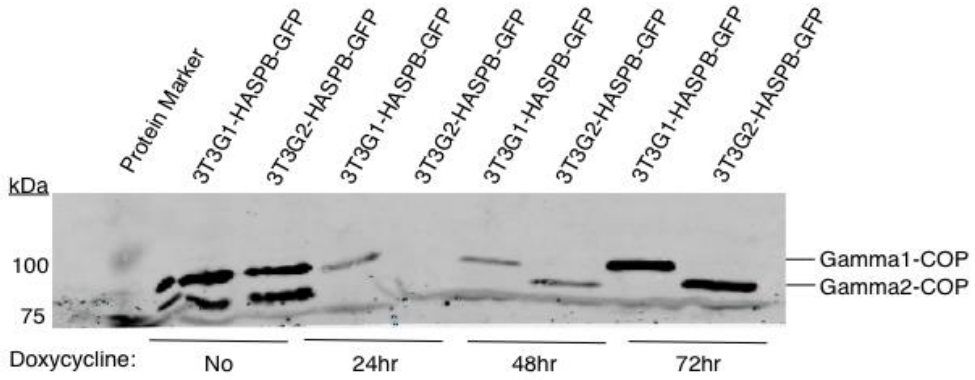

FIGURE 3: Immune-precipitation of γ1- and γ2-COP proteins from 3T3g1- and 3T3g2-HASPB-GFP cell lines. 500 µg total protein of doxycycline treated cell lysates were immune-precipitated with CM1-antibody (recognizing native coatomer). Due to a technical error, only 25% of the 24 h and 48 h samples were loaded to 6% SDS-PAGE gel and analyzed by western blotting with a gamma-r antibody (recognizing γ1-COP and γ2-COP).

As shown in Figure 3, uninduced cells express both γ1- and γ2-COP subunits in similar amounts. On the other hand, the doxycycline treated cell lines exhibit expression of only one of the subunits. The amount of protein appears to be increased after 72 h of induction; which is due to a loading error. This result shows that the characteristics of the template cells remained while the stable cell lines were co-expressing HASPB-GFP.

3.1.3. siRNA knockdowns of coatomer subunits in HeLa cells

HeLa SH4-HASPBN18-GFP/SH4-YesN18-Cherry Clone#5 (HeLa double5) stable cell lines, which in a doxycycline dependent manner simultaneously express fluorescently tagged HASPB and Yes were provided by Dr. Julia Ritzerfeld. Preliminary data from the Nickel Laboratory indicated that SH4 domain containing reporter proteins accumulated in perinuclear regions instead of locating to the plasma membrane, when γ2-COP was knocked down in HeLa double5 cells. This implied that proper targeting of these unconventionally secreted reporter proteins could depend on one of the γ-COP subunits. Therefore the intracellular localization of the SH4-proteins was investigated.

3.1.3.1. Effect of β, δ and α subunits on transport of SH4-proteins

HeLa double5 cells were treated with doxycycline for 24 h and then transfected with siRNAs directed against various coatomer subunits. Scrambled siRNA and siRNA against GFP were used as controls, as well as mock treatment and non-treated cells. After transfection, cells were split for biochemical and microscopic analysis to determine knockdown efficiency. Cells were lysed with lysis buffer containing 1% TritonX100. 60 µg of cell lysates were loaded in each lane of 4-12% Bis-Tris Nu-PAGE gel. Western blot was performed using antibodies against coatomer subunits, GFP and, as loading control, against GAPDH.

β- and δ-COP siRNA transfections are shown in Figure 4. Untreated and mock treated cells showed comparable levels of β-, δ-COP and GFP protein. The housekeeping protein GAPDH was chosen as loading control for all lanes. With GFP siRNA, serving as positive control, 90 percent of the protein was silenced. With siRNAs targeting β- and δ-COP, the respective protein levels were significantly decreased (Figure 4, red star), while the control samples (scrambled, GFP siRNA and mock, non-treated cells) did not show altered protein levels of the coatomer subunits. In addition, when β-COP was knocked down, δ-COP levels also decreased. Since coatomer is a multi-protein complex, down regulation of one subunit (β-COP) also caused a loss of another subunit (δ-COP). Taken together, siRNA knockdowns of β- and δ-COP resulted in significant depletion of the respective proteins.

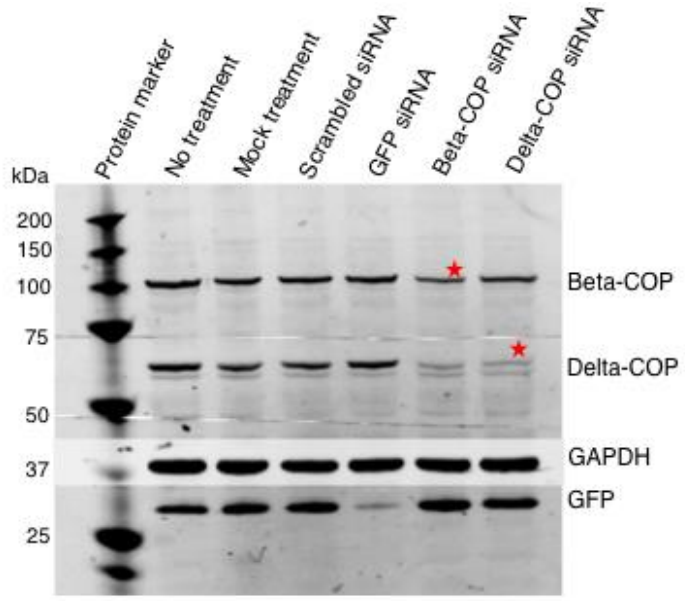

FIGURE 4: β- and δ-COP siRNA knockdown of HeLa double5 cell line. siRNA knockdown cells were lysed and 60 µg protein was loaded in each lane of the 4-12% Bis-Tris Nu-PAGE gel. Western blot was performed using antibodies against β-COP, δ-COP, GAPDH and GFP.

Quantification of the knock down is shown in Figure 5. All bands were normalized first to the loading control and then to the mock treated cells. The normalized results show 60-80% decrease in the amount of the targeted protein. A similar knockdown efficiency of coatomer subunits was observed in repetitions of the experiments (n=7).

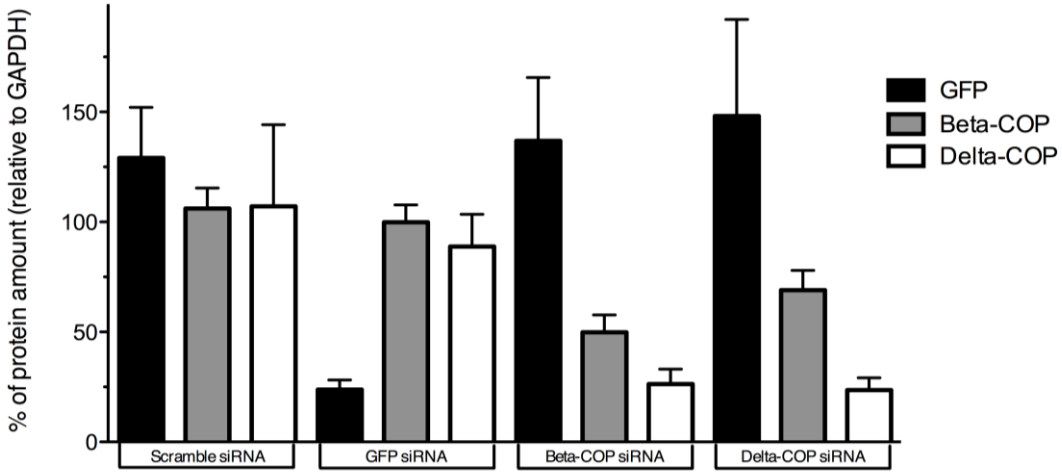

FIGURE 5: Quantification of siRNA knockdown in HeLa double5 cell line. HeLa cells were knockdown with siRNAs against GFP, β-COP and δ-COP. Mock treatment and scrambled siRNAs were used as negative controls. All the bands were normalized to the loading control GAPDH first, and then to the mock treatment (Figure is a representative of n=7)**.**

In addition to the biochemical analyses, cells were prepared for microscopy. Fixing the cells with different concentrations of paraformaldehyde (PFA) resulted in loss of fluorescence; therefore cells were imaged live by confocal microscopy. As also shown by western blot, GFP fusion protein expression was down regulated by the GFP siRNA (Figure 6, G). In untreated cells, SH4-proteins HASPB and Yes localized to the plasma membrane and the same was observed for mock and scrambled siRNA treated cells. Transfection with β- and δ-COP siRNAs, however, resulted in perinuclear accumulation of HASPB-GFP, while Yes-mCherry was localized mainly to the plasma membrane. Furthermore, β- and δ-COP siRNA transfected cells displayed altered cell morphology: cells were more elongated in comparison to control cells (Figure 6). Additionally, a siRNA knockdown against α-COP was performed. This knockdown resulted in down regulation of α-COP, and resulted in perinuclear accumulation of HASPB, while Yes was mainly localized to the plasma membrane (data not shown).

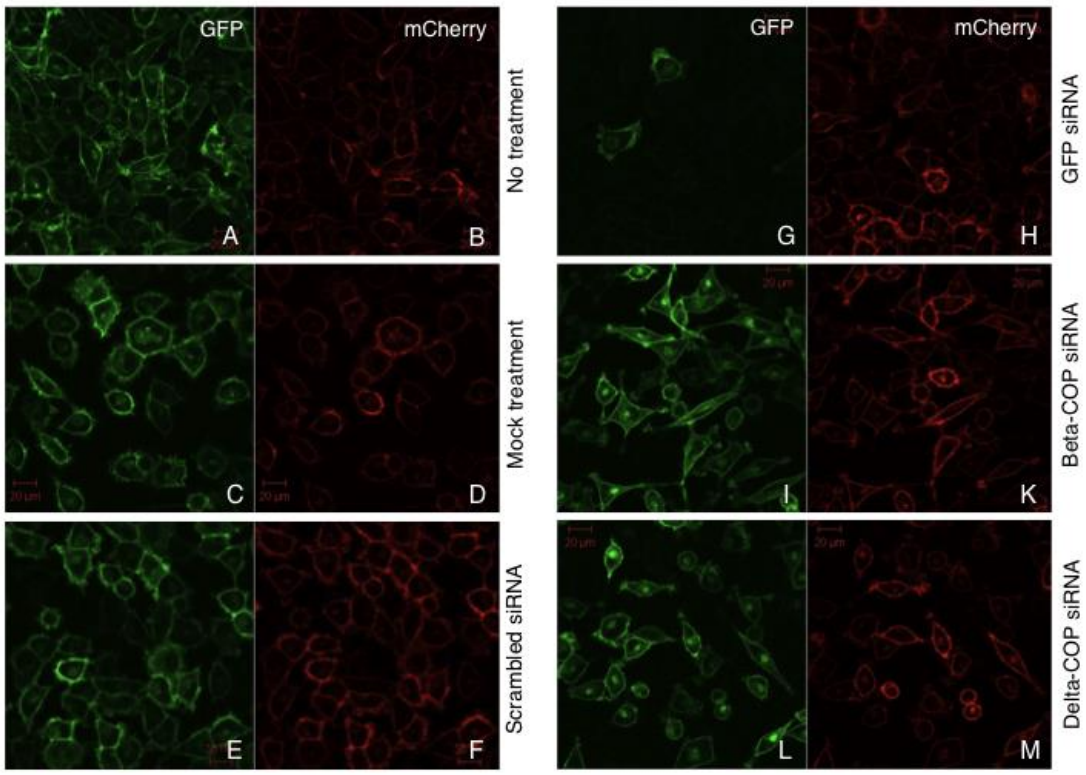

FIGURE 6: Immunofluorescence of siRNA knockdown HeLa double5 cells. Cells were treated with siRNAs against the subunits of the coatomer indicated and induced with doxycycline for expression of the reporter proteins. Following 24 h induction cells were visualized by confocal microscope.

3.1.3.2. Effect of different ζ-COP isoforms on transport of the SH4-proteins

As preliminary data from the Nickel Laboratory implied, only one of the γ subunits of coatomer was affecting the transport of the SH4-proteins to the plasma membrane. In order to probe isoform specific effects on the transport of the SH4-porteins, other isoform specific coatomer subunits ζ1- and ζ2-COP were investigated.

ζ1-COP and ζ2-Cop siRNA knockdown experiments were performed according to the same protocol and blotted for GAPDH, GFP, ζ1- and ζ2-COP antibodies. As depicted in Figure 7, the GAPDH amount indicates comparable loading of all lanes. Treatment with GFP siRNA resulted in more than a 90% reduction in the level of GFP protein. ζ1-COP level was already low in the control cells. Upon siRNA treatment a 70% reduction of ζ1-COP was observed. Surprisingly, ζ2-COP was not detectable in HeLa double5 cells.

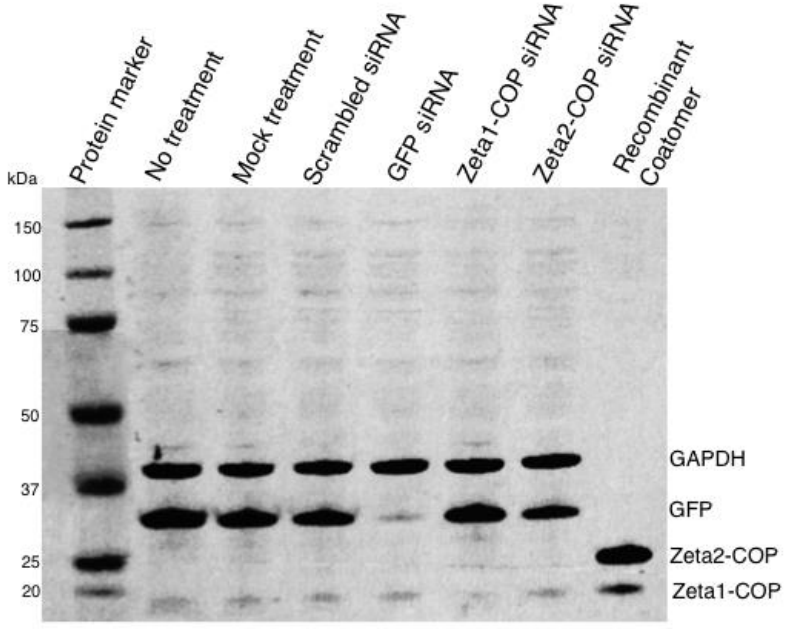

FIGURE 7: siRNA knockdown of ζ-COP subunits in HeLa double5 cell line. siRNA knockdown cells were lysed and 60 µg of protein was loaded in each lane of 4-12% Bis-Tris Nu-PAGE gel. Western blot analysis was performed using antibodies against GAPDH, GFP and Zeta-r (recognizing both ζ-COP subunits).

Therefore, quantitative real time PCR (qRT-PCR) was performed to quantify the mRNA level of ζ2-COP, indicating that HeLa double5 cell lines contain only neglectable amounts of ζ2-COP mRNA (Figure 8), while the positive controls HepG2 and HEK293T cells show 42 and 10 fold higher quantities of ζ2-COP mRNA, respectively.

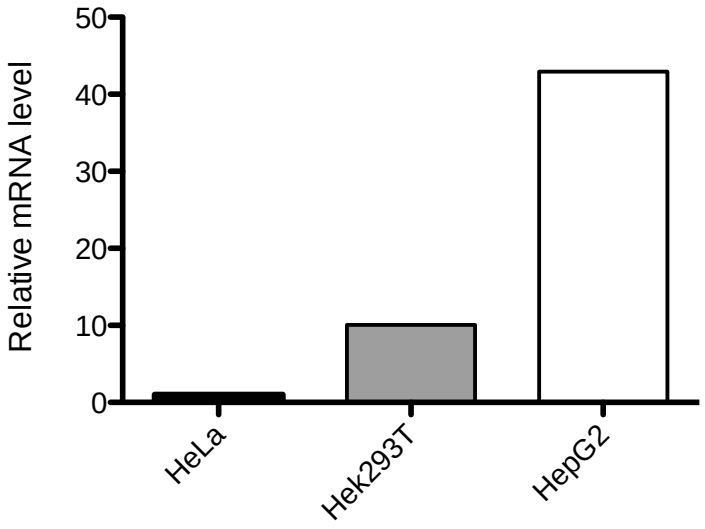

FIGURE 8: Relative quantification of ζ2-COP mRNA levels. RNA was isolated from HeLa, Hek293-T and HepG2 cell lines and subjected to RT-PCR. Relative amounts of mRNA levels for ζ2-COP are compared.

3.1.3.3. Effect of γ-COP isoforms on the transport of SH4-proteins

To investigate the effect of γ subunits on the transport of the SH4-proteins, HeLa double5 cells were transfected with siRNAs against γ subunits of coatomer. For γ1-COP, three different siRNAs were used: G1-115, G1-116 and G1-si (Table 3). Cell lysates were subjected to 6% SDS-PAGE gels with a Bisacrylamide to Acrylamide ratio of 1:100 (instead of the usual 30%) for better separation of γ1- and γ2-COP. Western blots were performed using antibodies against γ-COP (anti-gamma-r) and α-COP (anti-alpha-COP).

Figure 9 illustrates that untreated, mock treated and cells treated with scrambled siRNA display similar amounts of γ1- and γ2-COP. The recombinant coatomer sample shows similar amounts of protein in positive control treatments for the two γ-COP subunits (Figure 9, Lane 10). G1-116 and G1-si

siRNAs down regulated γ1-COP in the cells, while G1-115 siRNA was not affecting the γ1-COP amount in the cell (Figure 9, Lane 6-8). In the case of γ2-COP, G2-si siRNA down regulated the protein successfully (Figure 9, Lane 9). The knocked down cells were subjected to microscopy for possible effect on their phenotype.

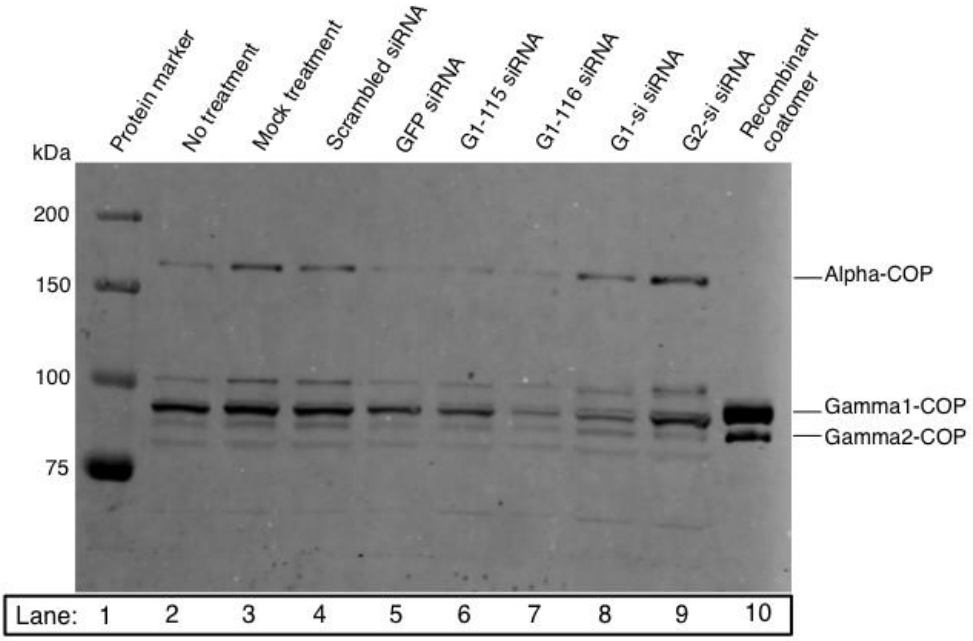

FIGURE 9: γ-COP siRNA knockdown in HeLa double5 cell line. Cells were treated with different siRNAs against γ subunit of coatomer for 48 h. Cell lysates were loaded on 4-12% Bis-Tris Nu-PAGE gel. Western blot was performed using antibodies against γ subunit (gamma-r antibody recognizing γ1- and γ2-COP) and α subunit.

Cells were also analyzed by microscopy to visualize the effect of both ζ- and γ-COP siRNA knockdowns. As depicted in Figure 10, cell morphologies of mock and scrambled siRNA treated cells were indistinguishable from the control cells. HASPB-GFP and Yes-mCherry localized mainly to the plasma membrane (Figure 10, A-D). However, transfection with ζ1-COP siRNA severely altered the morphology (Figure 10, E-F). Cells were elongated and an accumulation of HASPB-GFP in the perinuclear region was observed (Figure 10, E). However, Yes-mCherry localization to the plasma membrane was not compromised in the absence of ζ1-COP (Figure10, F). Since no ζ2-COP was detectable in HeLa double5 cell lines, knockdown of ζ1-COP results in retention of the HASPB-GFP. Accordingly, ζ2-COP siRNA knockdown cells were not affected, i.e.

HASPB-GFP and Yes-mCherry were localized to the plasma membrane (Figure 10, E-H). γ1-COP siRNA knockdown cells were not morphologically altered and transport of the reporter proteins to the plasma membrane was not affected by the knockdown (Figure 10, I-P). G1-115 siRNA knockdown shows a very low amount of accumulation of the SH4-proteins at the perinuclear region, but compared to mock treatment and scrambled siRNA controls it was not significantly altered (Figure10, I-J). Likewise G2-si siRNA knockdown shows no phenotype (Figure 10, O-P).

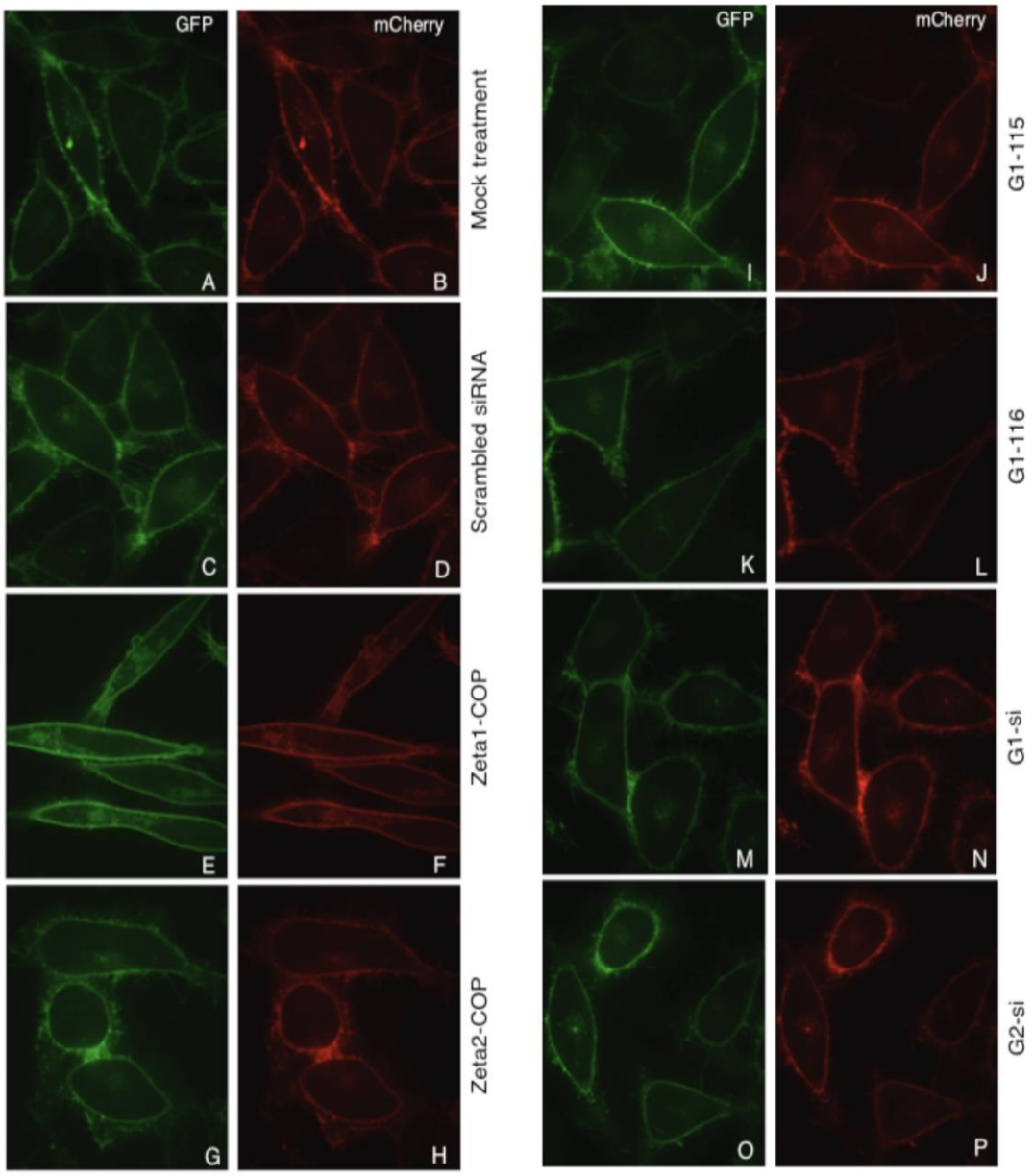

FIGURE 10: γ- and ζ-COP siRNA knockdown in HeLa double5 cell line siRNAs against γ- and ζ-COP subunits of coatomer were used to knock down the respective proteins in HeLa cells, and the cells were analyzed by fluorescence microscopy.

Altogether, knockdown of common coatomer subunits resulted in pronounced retention of the SH4-HASPB-GFP at the perinuclear region, suggesting that coatomer is involved in the transport of the SH4 domain containing reporter protein HASPB to the plasma membrane. However, knockdown of either γ1- or γ2-COP subunits do not individually affected the transport of reporter proteins.

3.2. CHAPTER II: Impact of Brefeldin A analogues on Golgi morphology

The chemical compound Brefeldin A (BFA) has been established in preventing transport by blocking the assembly of vesicular coats (Berger et al., 1993; Helms and Rothman, 1992a; Klausner et al., 1992; Lippincott-Schwartz et al., 1990). The molecular target of BFA is the guanine exchange factor (GEF) interaction with Arf1. This interaction is important in cancer research as it is highly cytotoxic (Ohashi et al., 2011). Analogues of this compound were synthesized by the Helmchen Laboratory (Department of Chemistry, Heidelberg University). This chapter describes the effect of these analogues in mammalian cells in comparison to the original Brefeldin A.

3.2.1. Effect of six novel Brefeldin A analogues in mammalian cell lines

Initial experiments with BFA analogues are listed below (Table 5) and their chemical properties were described in detail in “Synthesis and Biological Properties of Novel Brefeldin A Analogues” (Förster et al., 2011).

HeLa cells were used to monitor effects of BFA analogues on Golgi morphology. Cells were treated either with BFA or its analogues for 30 min and 60 min at 37°C. Subsequently, the cells were incubated for 2 h in fresh medium after the treatment, in order to test for the reversibility of effects on the Golgi. Cells were subjected to immunofluorescence labeling with the *cis*-Golgi marker anti-GM130 and analyzed by spinning disk confocal microscopy.

Brefeldin A	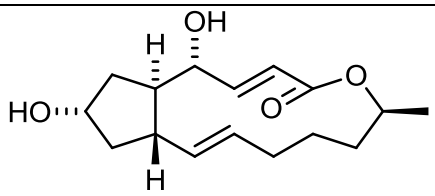

No	Name of the analogue	Structure of the analogue
1	(6R)-Hydroxy-Brefeldin A	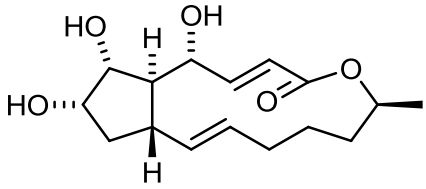
2	(7S)-Amino-Brefeldin C	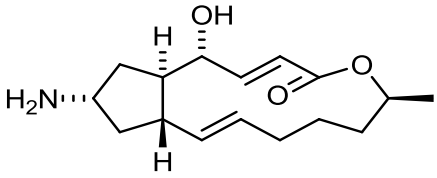
3	SF692	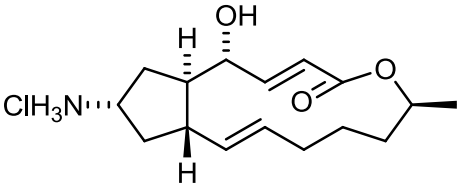
4	SF687	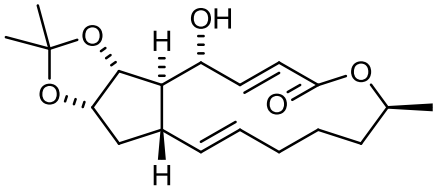
5	Brefeldin A-Lactamanalogue	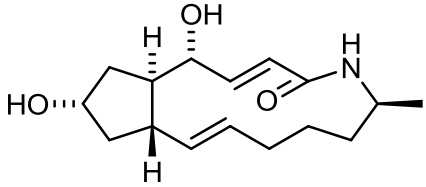
6	Brefeldin C-Lactamanalogue	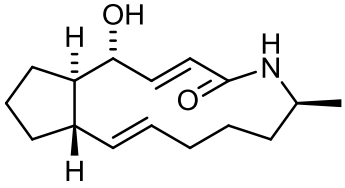

TABLE 5: Brefeldin A and the analogues

When cells were treated with the compounds for 30 min, BFA treated cells show a disrupted Golgi apparatus, while control cells maintain an intact Golgi (Figure 11). Similar Golgi disruption effects were observed with (6R)-hydroxy-BFA and BFA lactam analogue. At this time point, (7S)-amino-BFC, SF692, SF687, and BFC lactam analogues showed no effect on Golgi morphology.

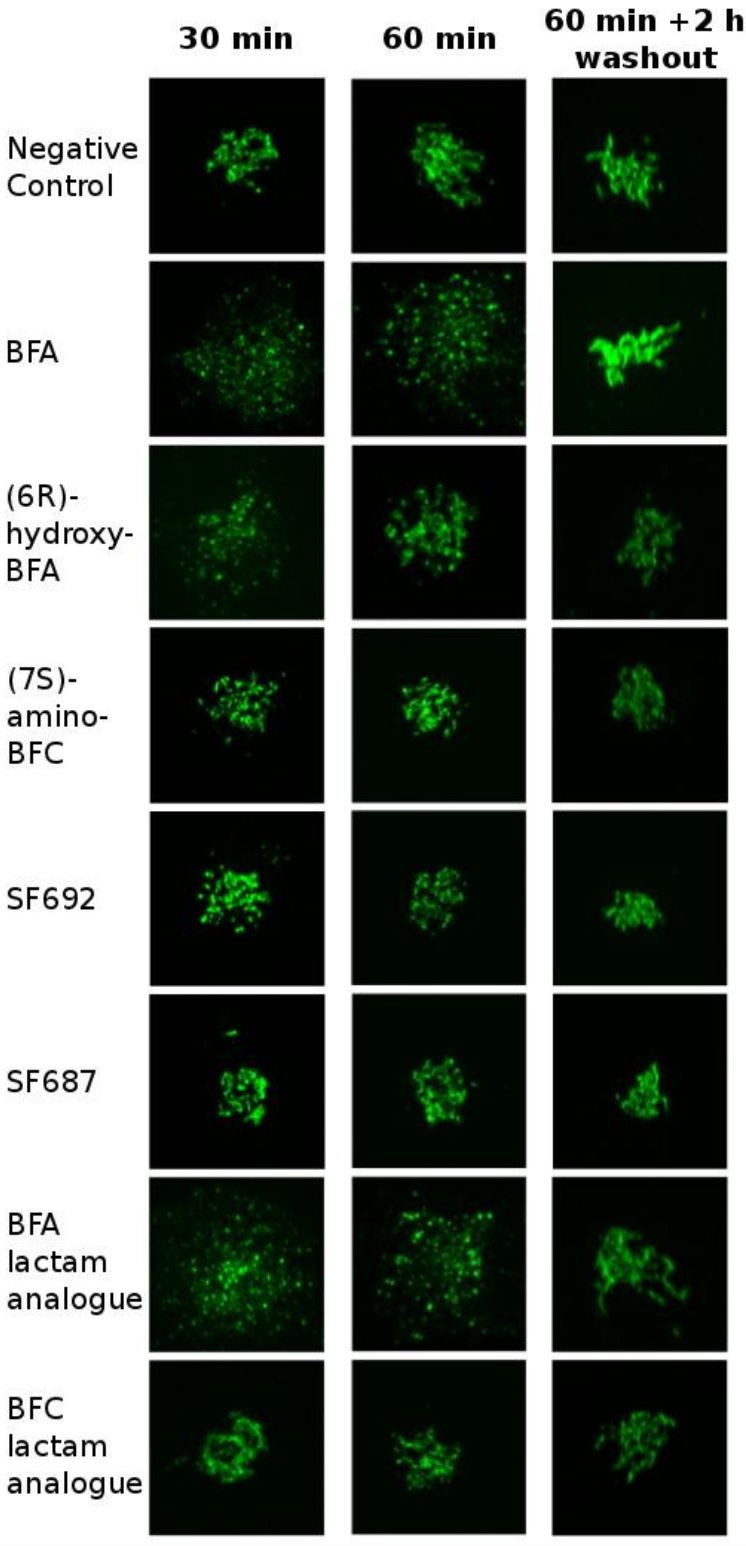

FIGURE 11: Treatment of HeLa cells with Brefeldin A and the analogues. Cells were incubated with 1 µg/ml BFA and the analogues for the indicated times. As control, cells were incubated in medium without serum. Washouts were performed for 2 h in fresh medium after a 60 min incubation in the presence of the compounds. Golgi structure was visualized by the *cis*-Golgi marker anti-GM130 antibody.

When the time of exposure to the same (1 µg/ml) concentration of compound was extended to 60min, Golgi disruption effect was observed for (6R)-hydroxy-BFA and BFA lactam analogue (Figure 11). Other derivatives at this concentration showed very weak effects or did not affect Golgi morphology at all.

After 60 min treatment, the compounds were washed out for 2 h to probe for reversibility of the phenotypes. Golgi reassembly was observed in cells treated with (6R)-hydroxy-BFA and the BFA lactam analogue. The recovery of the Golgi disruption was slightly better for the BFA lactam analog in comparison to the BFA. All fluorescence micrographs are depicted in Figure 11.

Therefore, two substances, namely (6R)-hydroxy-BFA and BFA lactam analogue induce Golgi disassembly while the other four substances had no effect on Golgi morphology at 1 µg/ml after 30 min of treatment. The same two substances were also inducing Golgi disruption after 60 min, while the others did not. Following a 2 h washout, BFA lactam analogue resulted in a slightly better recovery then the (6R)-hydroxy-BFA. Following the washout, BFA lactam analogue treated cells were able to reverse the morphological changes in the Golgi at a level comparable with BFA.

3.2.2. Effect of four novel Brefeldin A analogues in mammalian cell lines

A second round of experiments were performed in collaboration with the Helmchen Laboratory with newly synthesized BFA analogues. Compounds were named as listed below (Table 6) and their chemical properties were described in detail in the manuscript “Synthesis and Biological Properties of Novel Brefeldin A Analogues” (Seehafer et al., 2013).

HeLa cell lines were used again to observe effects on Golgi morphology. Cells were treated with BFA or analogues at a concentration of 5 µM for 30 min, 60 min and a 2 h washout after the 60 min treatment. Effects were visualized with immunofluorescence microscopy.

Brefeldin A	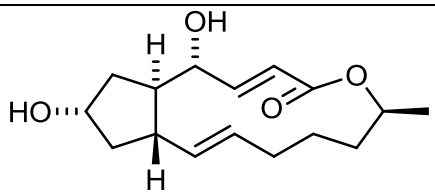

No	Name of the analogue	Structure of the analogue
1	5	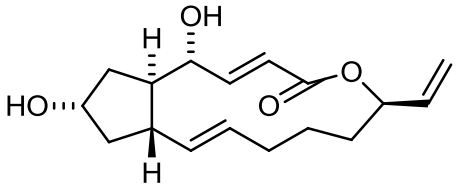
2	39a	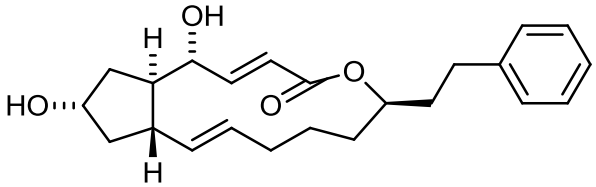
3	39b	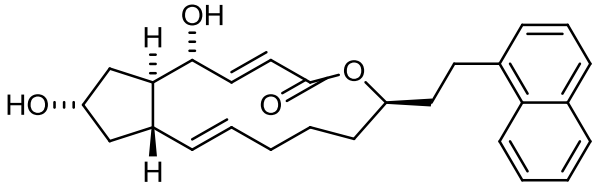
4	39e	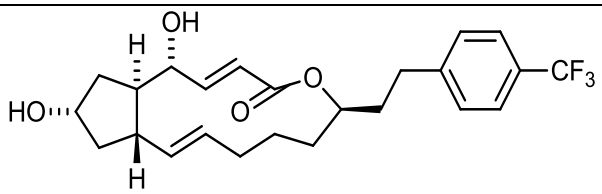

TABLE 6: Brefeldin A and the analogues

When the compounds were added to the cells for 30 min and the Golgi morphology was analyzed, all new compounds showed a partial Golgi disruption effect comparable to BFA (Figure 12). When the treatment was extended to 60 min for all compounds tested Golgi disassembly was observed, as shown in Figure 12.

The Golgi reassembly capability was investigated after a 2 h compound washout with fresh medium after the 60 min treatment, shown in Figure 12. While Brefeldin A treated cells were able to recover after 2 h of washout, almost no recovery was observed in the cells treated with compound 5. Compound 39a and 39b showed reassembly in almost only half of the cells. However the

compound 39e displayed a Golgi reassembly in a similar manner to Brefeldin A.

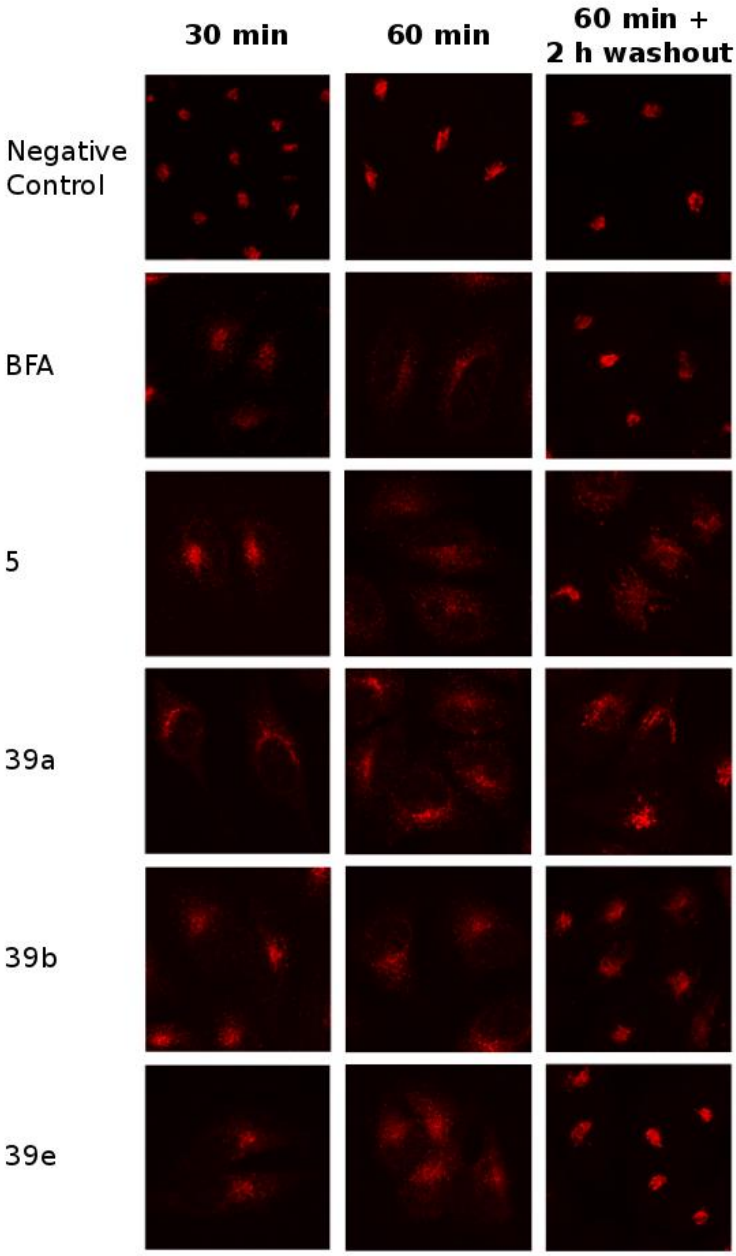

FIGURE 12: Treatment of HeLa cells with Brefeldin A and the analogues. Cells were treated with 5 µM final concentration of the compounds for the times indicated or mock treated. 2 h washout experiments were performed after 60 min treatment with the compounds. Golgi structure was visualized by the *cis*-Golgi marker anti-GM130 antibody.

In summary, all the compounds were capable to affect Golgi morphology by total disruption. In addition, compound 39a and 39b were allowing a partial reassembly after washout, whereas only compound 39e was able to fully recover the disassembly effect of the substance.

3.3. CHAPTER III: Oligomerization of p24 and p24L17F transmembrane domains

One of the major players of COPI coated vesicles are transmembrane proteins p24 family members. p24 family members form dimers and heterooligomers in addition to their monomeric forms. This equilibrium between inactive monomeric form and active oligomeric form of the p24 family members is suggested to be regulated by specific binding of SM 18 to the transmembrane segment of p24, as it was shown *in vitro* (Contreras et al, 2011). In order to test for the impact of SM 18 to p24, non-SM18 binding p24 variant (p24L17F) and wild-type p24 (p24 wt) were investigated *in vivo*.

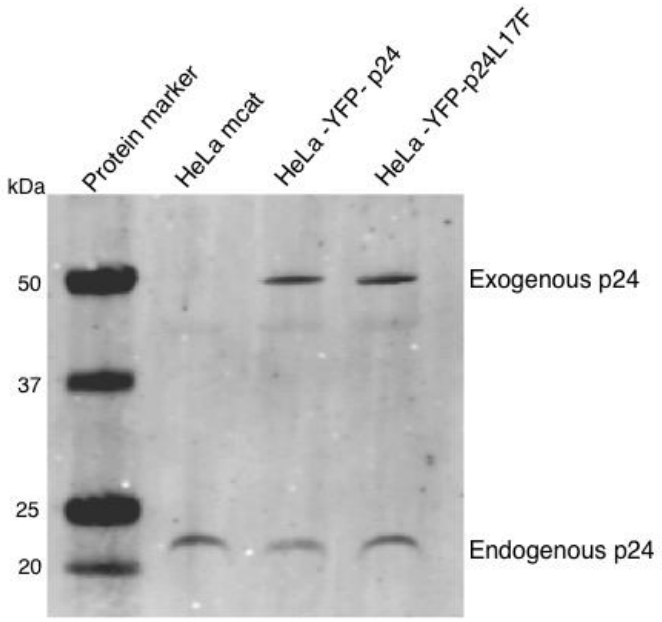

FIGURE 13: Western blot analysis of the expression of recombinant proteins. Stable HeLa cell lines were lysed after 24 h induction with doxycycline and western blot analyses was performed using an anti-p24 antibody (Elfriede, (Gommel et al., 1999)).

HeLa cells expressing YFP tagged p24 wild-type and p24L17F transmembrane domains in a doxycycline inducible manner were generated by Andreas M. Ernst. Since overexpression of the p24 family members results in mislocalization of the proteins, it was critical to determine the exact expression levels. To this end, cells were treated with doxycycline for different amounts of time to monitor exogenous expression in comparison to the endogenous

protein levels. For cell lysis, different detergents were evaluated to optimize the solubilisation of the membrane proteins (data not shown). Optimal conditions were observed with lysis buffer containing 4% octylglucoside, in accordance with previously established protocols for the analysis of p24 proteins (Jenne et al., 2002). Lysates were subjected to western blot analysis.

As it is shown in Figure 13, HeLa mCAT cells were used as control, since these cells were the source of the stable cell lines. Endogenously expressed p24 protein in the HeLa mCAT cells was observed in the blot, while ectopic expression of the tagged proteins was only observed in HeLa-YFP-p24 and HeLa-YFP-p24L17F lysates, together with endogenous p24 protein.

After determining the expression of the recombinant p24 proteins, expression levels of these proteins were quantified after induction for 8 h and 24 h. After the incubation, cells were lysed and subjected to western blot analysis. The antibody against p24 protein (Elfriede, (Gommel et al., 1999)) was used for the western blot analysis, but the antibody also led to the detection of unspecific bands, evident in Figure 14. Endogenous p24 protein is observed in all the lysates together with p24 fusion proteins. Lysates of uninduced cells also show the p24 fusion proteins, which is probably due to leakage in the promoter. This leakage, however, can be ignored since it has no effect in the experimental set up and/or the outcome. When recombinant protein levels of uninduced cells are compared to those in induced cells (Figure 14, Lane 2 to 3, Lane 4 to 5, Lane 6 to 7, and Lane 8 to 9) there is a clear increase in the amount of fusion protein. Furthermore, doxycycline induction of protein expression for 8 h results in a lower increase in expression of the p24 fusion protein compared to the level of increase after 24 h induction. When p24 wt and p24L17F (lane 7 and 9) are analyzed after 24 hours of induction, the amount of endogenous and exogenous p24 protein expressions is comparable.

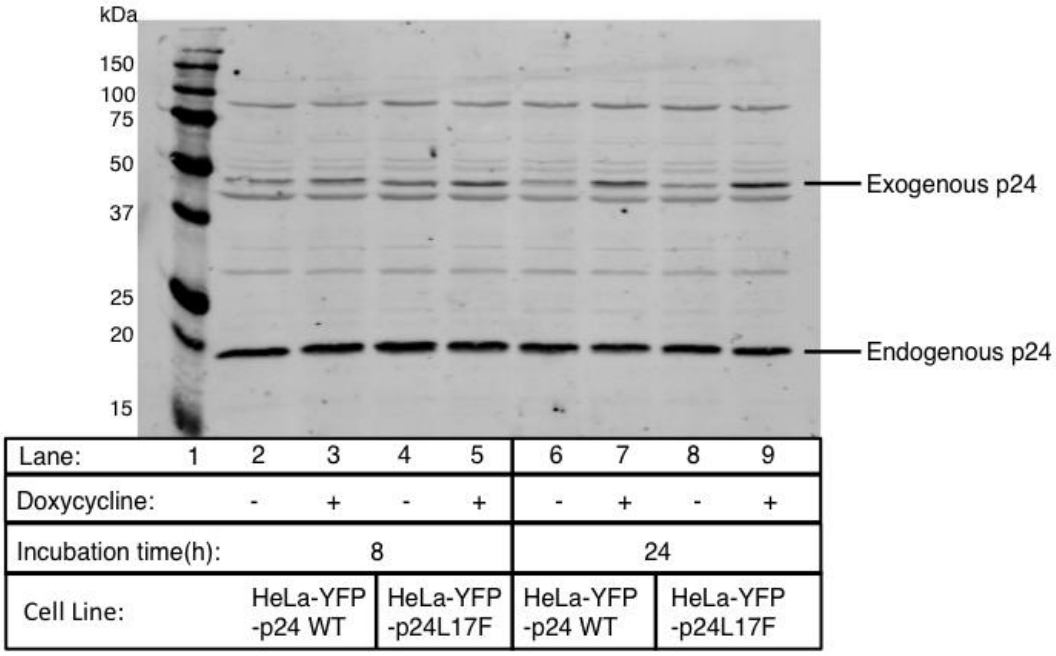

FIGURE 14: Different time points of induction for recombinant p24 expression in stable cell lines. HeLa-YFP-p24-wt and –p24L17F cell lines were lysed after 8 h and 24 h doxycycline induction and subjected to 4-12%Bis-Tris NuPAGE gel. Western blot analysis with an antibody against the p24 protein (Elfriede).

In order to monitor the degree of oligomerization of the p24 wt and p24L17F fusion proteins, *in vivo* crosslinking reagents were applied to the stable cell lines. Expression of recombinant proteins was induced by 24 h doxycycline incubation and cells were subjected to chemical crosslinking using the membrane-permeable, homobifunctional amine-reactive reagent disuccinimidyl glutarate (DSG; 0.5 mM in DMSO) for 15 min. Cross-linked products of p24 wt and p24L17F proteins were then analyzed by western blot. As shown in the Figure 15, control HeLa MCAT cells display only endogenous p24 protein and not cross links in the blot, while in the lanes with HeLa cells expressing p24 wt and p24L17F in addition the YFP tagged proteins are seen. In the experimental setups incubated with DSG cross-linker, YFP tagged p24 and p24L17F amounts are reduced and oligomerized cross-linked products are present with an apparent MW of 100 kDa and higher (Figure 15).

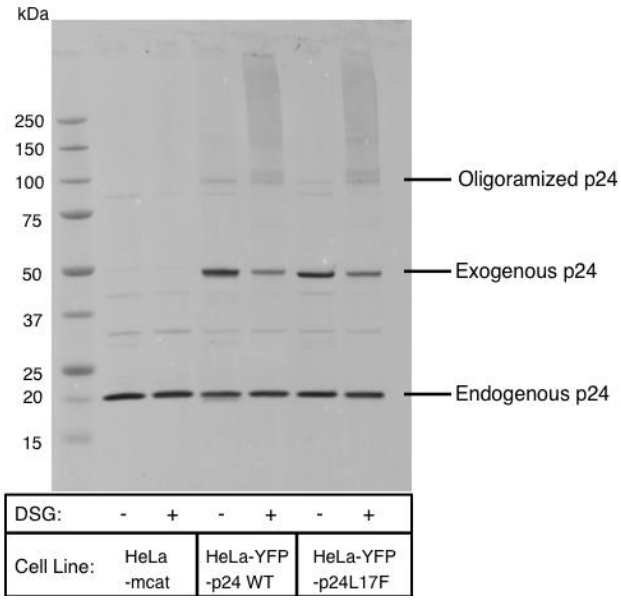

FIGURE 15: *In vivo* oligomerization of recombinant p24 proteins. After 24 h doxycycline induction, stable cell lines were incubated with 0.5 mM DSG cross-linker for 15 min. Cells were lysed and subjected to western blot analysis. Antibody against p24 (Elfriede) was used to label the membrane.

Cross-linked p24 wt and p24L17F proteins were quantified and compared as ratios to monomeric recombinant proteins, respectively. p24 wt oligomer/monomer ratios were set to 100% and compared to p24L17F oligomer/monomer ratios. YFP tagged p24 wt oligomer/monomer- and p24L17F oligomer/monomer-ratios were analyzed by two-tailed, paired t-tests as depicted in Figure 16.

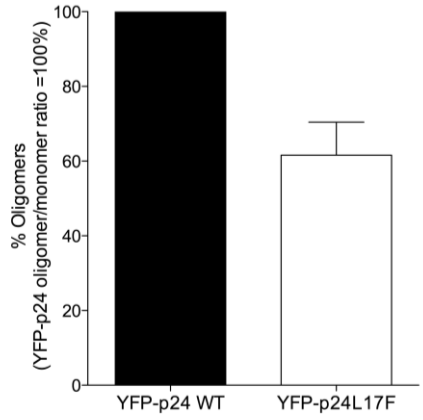

FIGURE 16: *In vivo* oligomerization propensity of HeLa cell lines stably transfected with YFP-p24 wt or YFP-p24L17F. YFP-p24 wt oligomer/monomer ratios were set to 100% (black bar; n=4) and YFP-p24L17F oligomer/monomer ratios are given as percentages hereof (white bar; 61.57% ±17.7 SD; n=4). YFP-p24 wt oligomer/monomer- and YFP-p24L17F oligomer/monomer-ratios were analyzed by two-tailed, paired t-tests (p=0.0165 (*)).

Binding of SM 18 was likely to be blocked via the single mutation at the transmembrane domain of the p24 protein (Contreras et al, 2012). As a result of *in vivo* chemically crosslinking of p24 wt and p24L17F, there is a significant shift in the equilibrium between oligomeric forms to the monomeric form of the non-SM 18 binding p24 protein.

3.4. CHAPTER IV: Kinetics of the p24 family members

3.4.1. Expression levels of the recombinant proteins

In order to address the kinetics of the p24 family members, one representative candidate from each group by virtue of their different travel rates; p23 and p24 was chosen according to the results of previous Wieland Laboratory member (Eva Emig, PhD thesis). Chinese hamster ovary (CHO) cell lines which express fluorescent-tagged p23 and p24 in a doxycycline-dependent manner were used. These cell lines were also used for the initial experiments. Cells were plated with 40% confluency. Plated cells were induced with doxycycline for 8 h and 24 h to confirm expression and compare the expression levels of the recombinant proteins. After the incubation, cells were lysed and subjected to western blot analysis using antibodies against p23 and p24 proteins. As shown in Figure 21, stably transfected CHO cell lines express endogenous p23 and p24 proteins, but expression levels of exogenous protein in increasing time points are not comparable between the two stable cell lines. The expression level of the recombinant protein from the CHO-YFP-p23 cell line is low compared to the expression of CHO-YFP-p24 cell line.

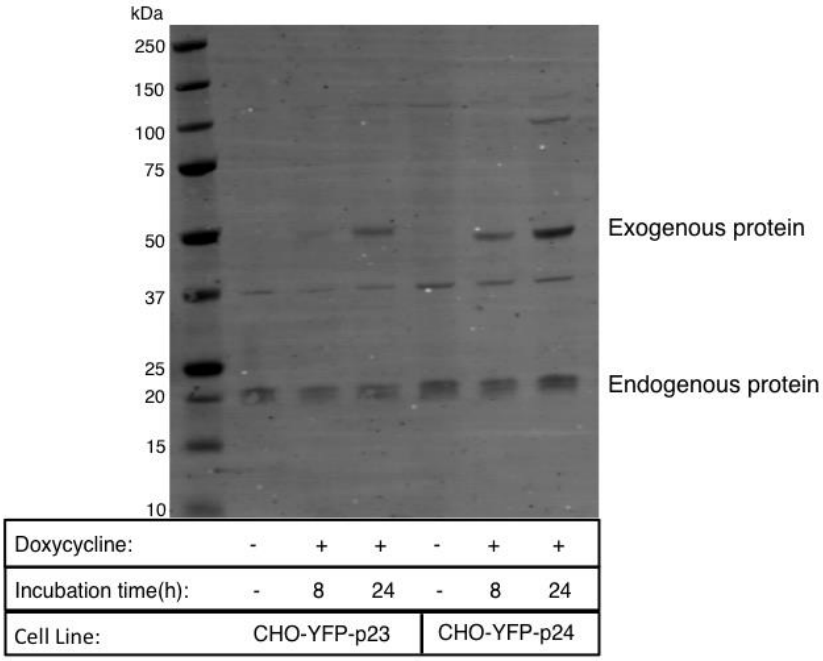

FIGURE 21: Expression levels of the stable cell lines after various induction times. CHO-YFP-p23 and CHO-YFP-p24 cell lines were incubated with doxycycline for 8 h and 24 h and lysed. 10% of the total cell lysates were subjected to 4-12% Bis-Tris NuPAGE gels. Western blot analysis was performed using anti-p24 (Elfriede) and -p23 (Henriette) antibodies.

In parallel, the same number of cells were plated and visualized through fluorescent microscopy. The expression level of recombinant p23 protein resulting from an 8 h induction was too low to be detected, thus cells were induced with doxycycline for 24 h. Surprisingly, the average expression level of p23 was not low; instead, the number of cells expressing recombinant protein was low (Figure 22).

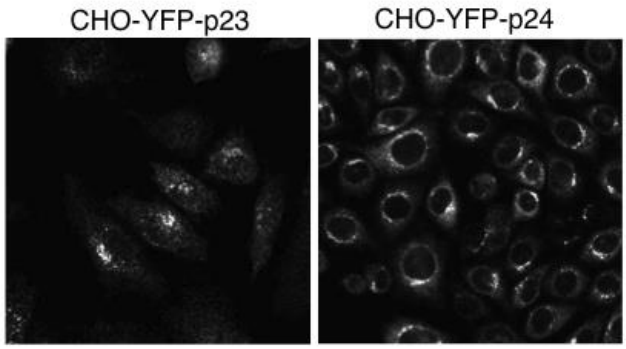

FIGURE 22: Expression of the recombinant p24 family members after 24 h doxycycline induction. CHO-YFP-p23 and CHO-YFP-p24 cell lines were induced for recombinant protein expression with doxycycline for 24 h and then visualized by microscope.

3.4.2. Localization of the recombinant proteins in the cell

Characterization of the CHO cell lines with immunofluorescence techniques was necessary to confirm the correct localization of the exogenously expressed tagged p24 family members compared to their endogenous counterparts. Taking into account the recombinant protein expressing cell number of the CHO-YFP-p23 cell line was not detectable after 8 h of induction, cells after 24 h induction were immune stained and the colocalization of the recombinant proteins was compared with the *cis*-Golgi marker GM130, the Endoplasmic Reticulum-Golgi Intermediate Compartment marker ERGIC53, and Endoplasmic Reticulum marker Calnexin.

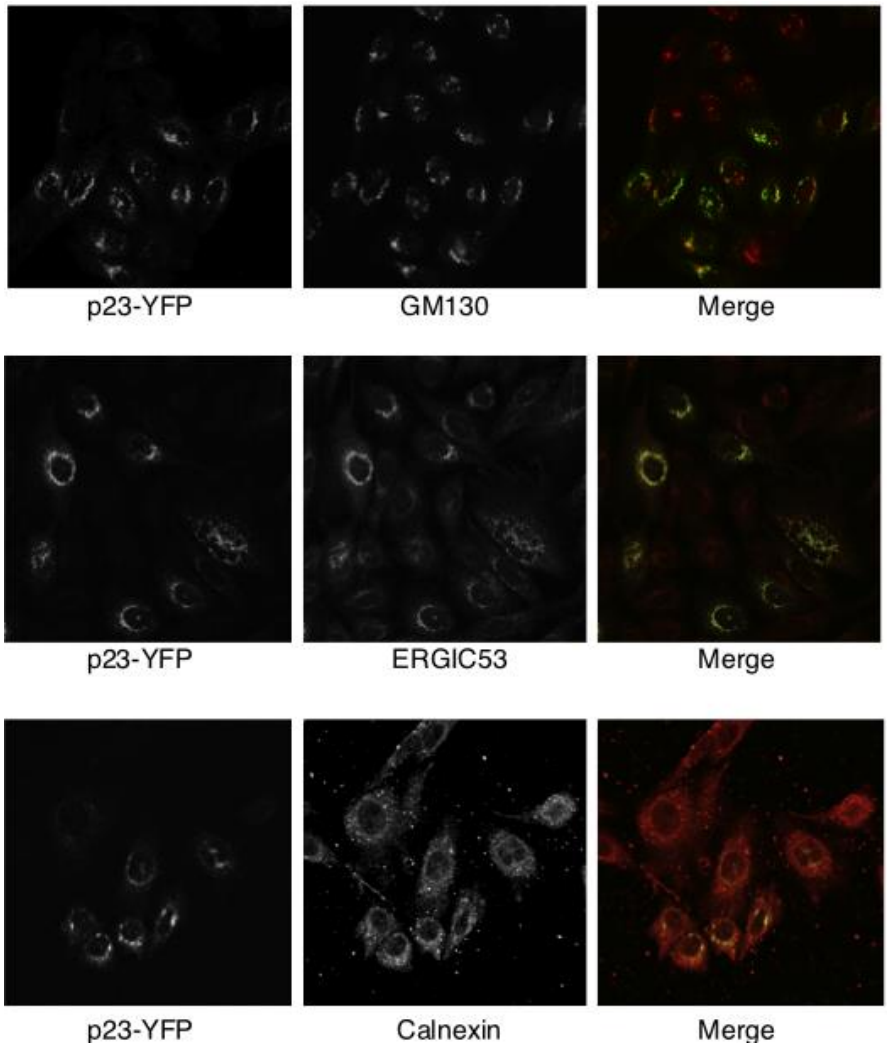

FIGURE 23: Colocalization of recombinant p23 protein in stable CHO cell lines. CHO-YFP-p23 cell lines were immune labeled for colocalization of the recombinant protein with various antibodies that immune label organelles in the early secretory pathway. Colocalization of YFP tagged p23 (yellow) with GM130, ERGIC53 and Calnexin (red) can be seen in the merge image (green).

Immune labelling of CHO-YFP-p23 expressing cell lines (Figure 23) implies a colocalization with Golgi, ERGIC and ER markers. Additionally, the number of cells expressing YFP-p23 is low when compared with the cells labeled with other markers (Figure 23, merge). The recombinant protein signal from CHO-YFP-p24 cell lines colocalizes with the ER, ERGIC and Golgi markers in the merged images (Figure 24). Furthermore, stable CHO cell lines were immune labelled with p23 and p24 antibodies to compare the localization of the exogenous protein versus endogenous protein. As a result, both recombinant proteins colocalize with the endogenous protein nicely (data not shown). Together these results are consistent with the fact that p23 and p24 proteins constantly cycle in the early secretory pathway (Gommel et al. 1999). In addition, the results determine the correct time interval for the induction of the exogenous protein expression since there was no accumulation of the exogenous protein in any compartment of the cell.

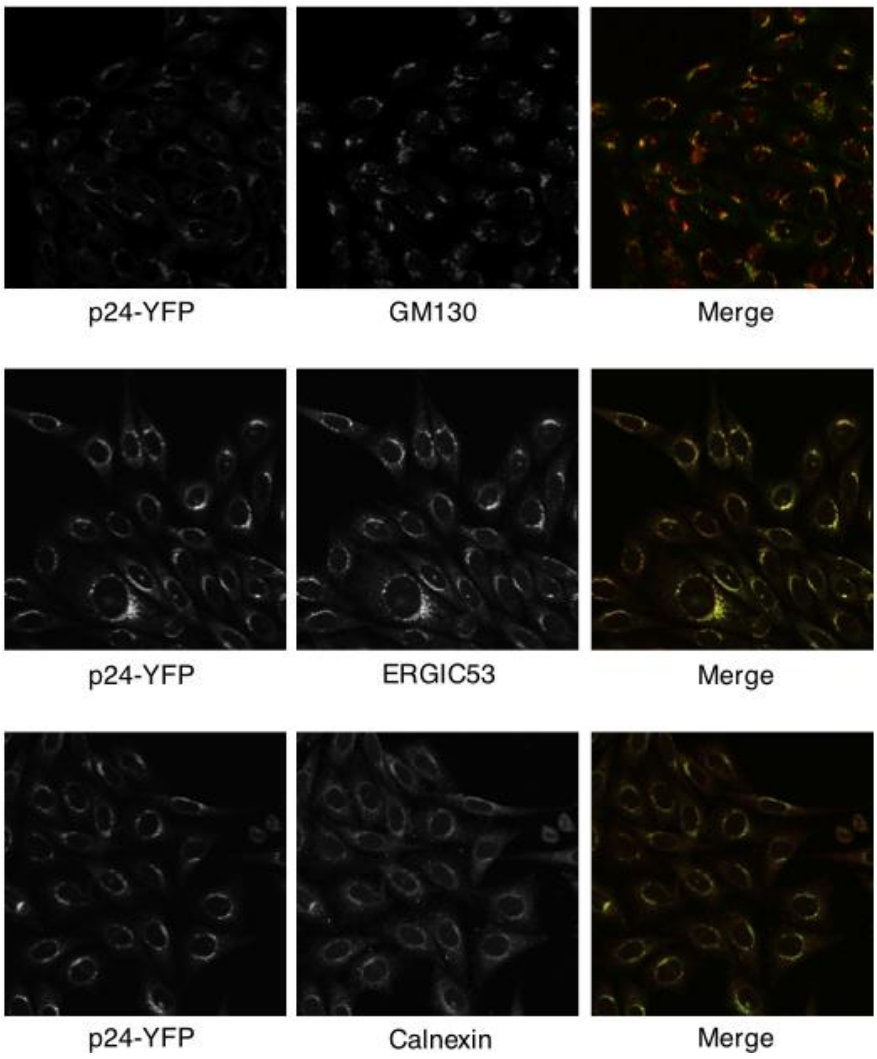

FIGURE 24: Colocalization of recombinant p24 protein in stable CHO cell line. CHO-YFP-p24 cells were subjected to immunofluorescence labeling with Golgi, ERGIC and ER markers for visualizing the colocalization. Colocalization of YFP tagged p24 (yellow) with GM130, ERGIC53 and Calnexin (red) is seen in the merged images (green).

3.4.3. Fluorescence Loss in Photobleaching of p24 family members

With FLIP the fluorescence intensity of a region of interests (ROI) is monitored while another ROI is bleached constantly. This allows to investigating if the two regions are connected and fluorescent proteins can move between them. This technique was used to monitor the fluorescence loss in the Golgi while bleaching parts of the ER to investigate the retrograde transport of the p24 family members (Phair and Misteli, 2001).

Stable CHO cell lines were tested for their suitability in Fluorescence Loss in Photobleaching (FLIP) experiments. One of the limiting factors is the heterogeneity of the recombinant protein expression in the two different cell lines. Therefore, the CHO-YFP-p23 cell line was subjected to Fluorescence-activated cell sorting (FACS) to collect a population of cells similar in expression to the CHO-YFP-p24 cell line. After the successful sorting, cells were subjected to FLIP experiments. However, despite several trials, CHO cell morphology was not suitable for the FLIP experiments, and the stable CHO cell lines could not be used for this experiment.

Instead of using CHO cells, p23 and p24 proteins were tagged with YFP and transiently expressed in HeLa cells. This system proved to be suitable for FLIP experiments.

The established method for Fluorescence Loss in Photobleaching (FLIP) was employed as conducted by Contreras et al. (2012) for the analysis of p24 proteins. Here, two Regions of Interest (ROI) of defined size were selected in each cell, parallel to each other, on both sides of the Golgi area. The distance between the ROIs and Golgi area as well as the sizes of the ROIs were determined in control experiments: The ROI's were placed at a certain distance to both sides of the Golgi area and moved closer each time to find regions that avoided bleaching of the Golgi ROI by the illumination beam. As an additional control, cells were fixed and subjected to the FLIP experiment. Once the area sizes and the positions were defined, live experiments were performed accordingly.

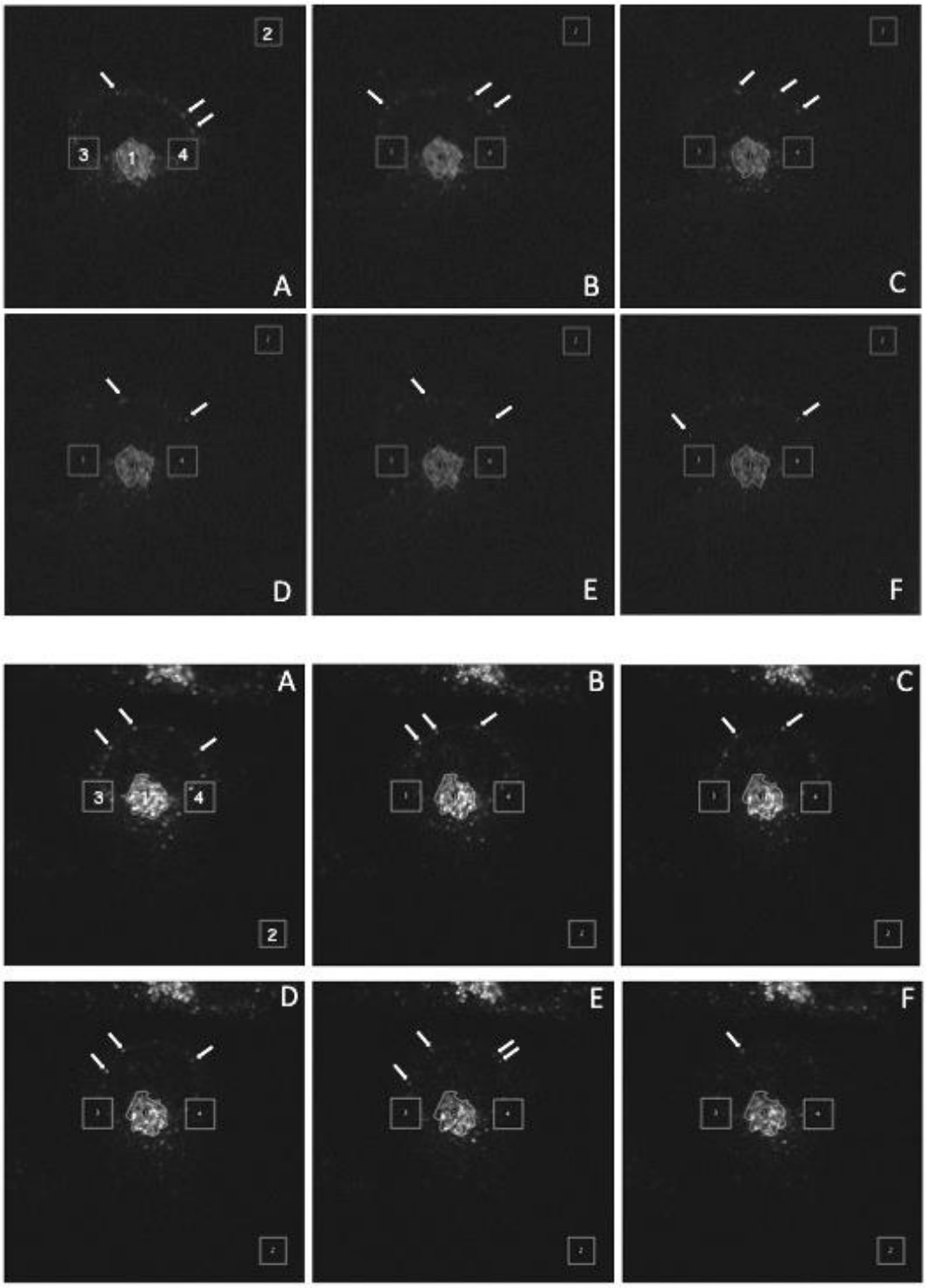

FIGURE 25: Sequence images from two FLIP experiments of HeLa cell lines transfected with YFP-p24. ROI #1 is within the Golgi area, ROI #2 is the background control, and ROI #3 and #4 are bleaching areas. Arrows points to the appearance of the YFP tagged proteins in different parts of the cell.

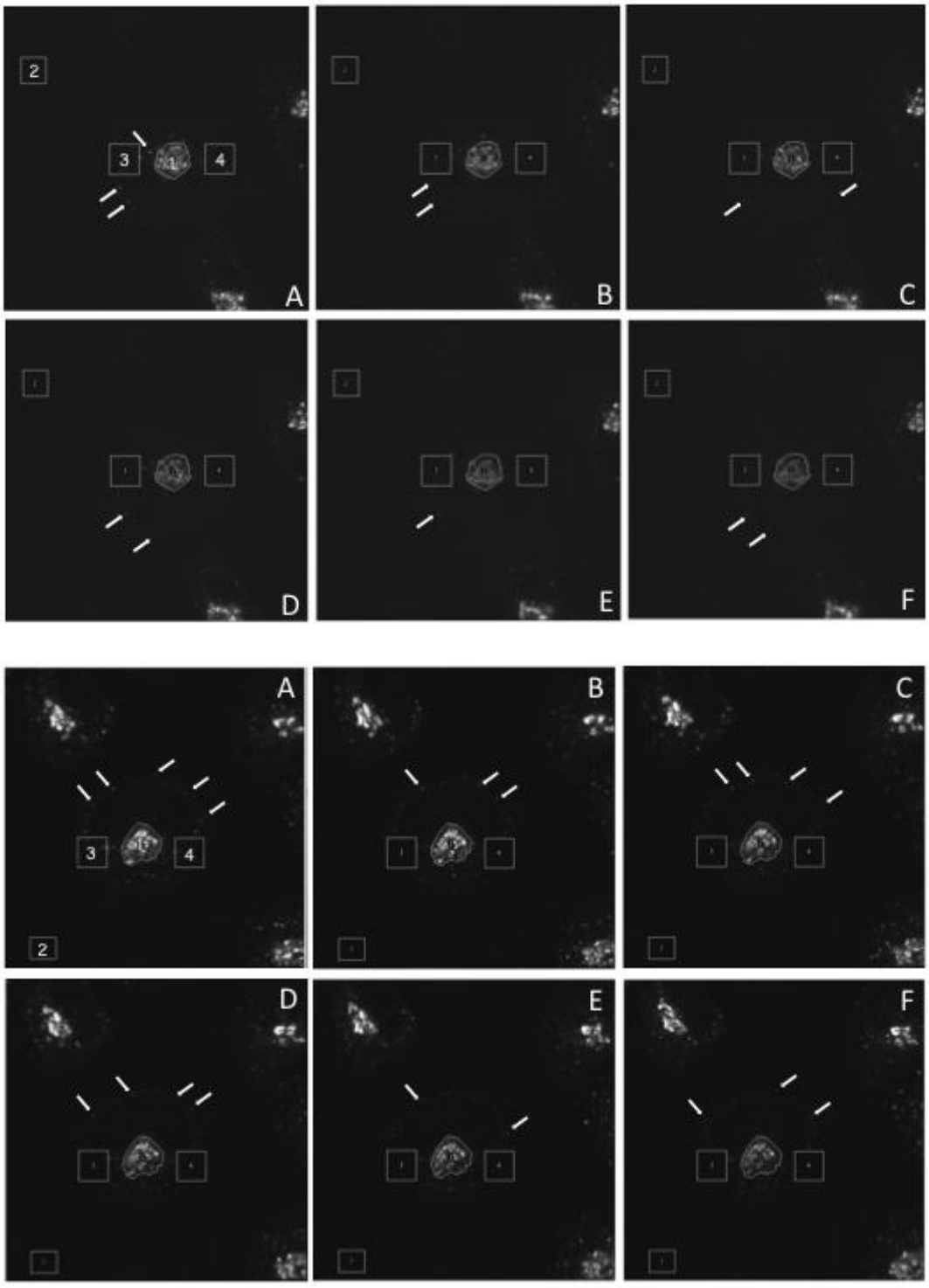

Figure 26: Sequence images from two FLIP experiments of HeLa cell lines transfected with YFP-p23. ROI #1 is within the Golgi area, ROI #2 is the background control, and ROI #3 and #4 are bleaching areas. Arrows points to the appearance of the YFP tagged proteins in different parts of the cell.

Figure 25 and 26 shows representative sequence images from examples of FLIP experiment where HeLa cell lines are transiently transfected with YFP-p24 and YFP-p23. ROI #3 and #4 are the bleaching ROI's and were placed in parallel. ROI #2 was used as a background control. ROI #1 was placed at the Golgi area. While ROI #3 and #4 were bleaching, the fluorescence intensity decreases in ROI #1 was monitored. As the YFP tagged p23 and p24 proteins cycle from Golgi ROI to bleaching ROI's and back, the fluorescent proteins were bleached and the total fluorescence intensity of the Golgi ROI decreased. Arrows in Figure 25 and 26 indicate additional protein transport activity as the fluorescent-tagged proteins appear and disappear in other regions of the cell during the sequence of images.

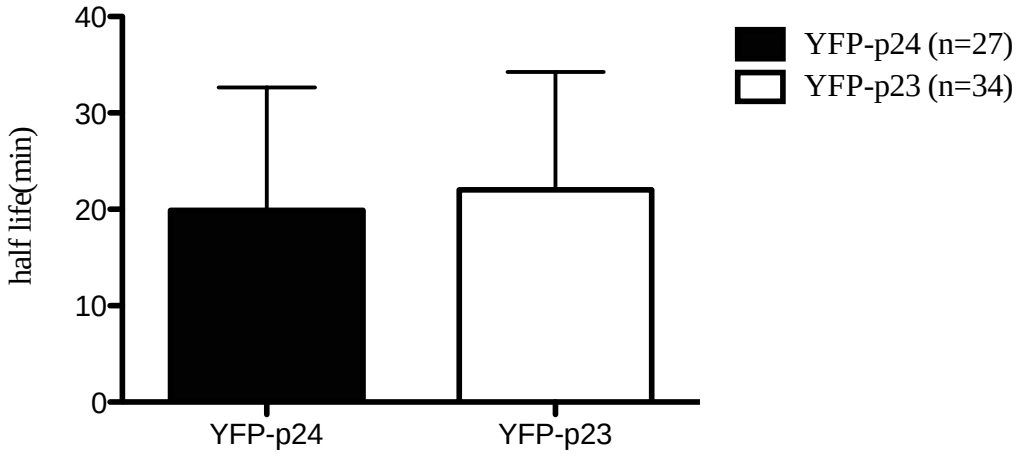

Half-life p23/p24: 1.10 ± 0.95 min

FIGURE 27: Quantification of the FLIP experiments. Average half lifes of the YFP-p23 and YFP-p24 fluorescence intensity are compared. P-value of two tailed, unpaired t test (>0.05) is presented. The number of individual experiments performed for YFP-p23 (n= 27) and for YFP-p24 (n=34) is given.

Quantification of the FLIP data is shown in Figure 27. Half-lifes of the two proteins fluorescent decays were calculated and compared. The difference of the half-lifes of YFP-p23 to YFP-p24 was not significant according to the two tailed unpaired t test.

3.4.4. Photoswitchable protein tag: Dronpa

In order to selectively follow up protein trajectories, another fluorescent tag was fused to p23 and p24 proteins as a reporter protein: the photo-switchable fluorescent tag, dronpa (Day and Davidson, 2009). There are several advantages of this novel GFP-like protein. The dronpa has a photo-activatable feature; it can be activated or deactivated with different wavelengths, repeatedly. Once it is activated at the region of interest, it is possible to follow the path of the tagged proteins as they are transported throughout the cell. Therefore, this technique is more sensitive and provides an additional method of obtaining protein transport rates.

After the constructs were created, the transient transfection of HeLa cells was optimized. Cells were transfected simultaneously for western blot analysis and visualization under the microscope.

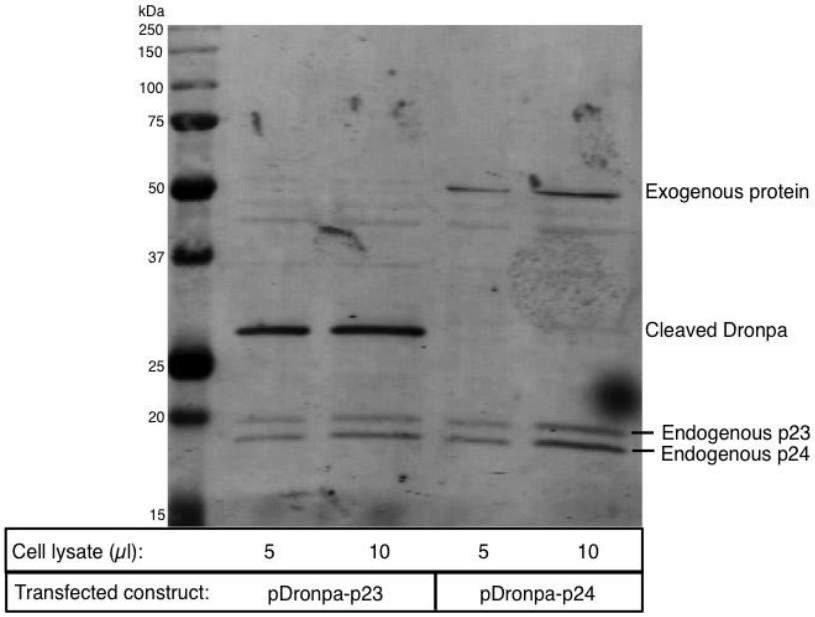

FIGURE 28: Transient transfection of HeLa cell lines with dronpa constructs. HeLa cells were transfected with dronpa constructs and subjected to western blot. 5% and 10% of the cell lysates were loaded on SDS-PAGE gel and labeled with antibodies against p24 (Elfriede), p23 (Henriette), and dronpa (GFP).

Transfected HeLa cells were lysed and increasing amounts of the cell lysates were subjected to western blot analysis with antibodies against p23, p24 proteins and dronpa (Figure 28). Transiently transfected cells with pDronpa-

p24 show both endogenous and exogenous proteins at the expected size. Nevertheless, pDronpa-p23 transfected cells show only the endogenous proteins at the expected size (20 kDa). The exogenous protein is not present in the blot. Besides, there is a strong band at the size of truncated dronpa. As DNA sequencing showed not stop codon between the dronpa tag and the p23 protein, it seems that pDronpa-p23 is degraded after transfection.

In order to directly visualize the constructs *in vivo*, transfected cells were observed by confocal microscopy. pDronpa-p23 transfected cells showed fluorescence predominantly in the cytosol as shown in Figure 29. pDronpa-p24 transfected cells, on the other hand, show perinuclear localization (Figure 29).

Together these findings show that the pDronpa-p23 has to be improved, while a pDronpa-24 construct was successfully created.

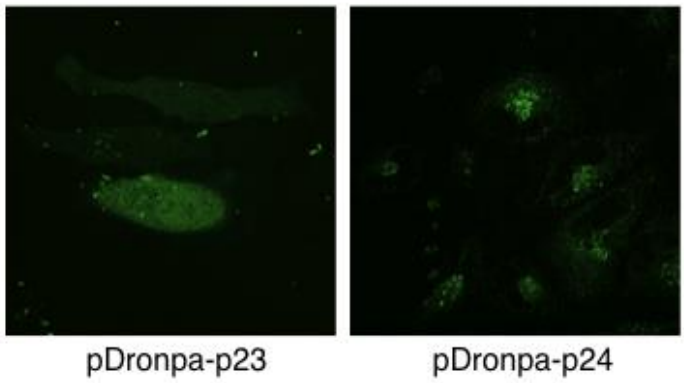

FIGURE 29: Microscope image of cells transfected with dronpa constructs. HeLa cells were transfected with pDronpa-p23 and pDronpa-p24 for 24 h and observed *in vivo*.

The functional pDronpa-p24 was investigated further. To this end, pDronpa-p24 transfected cells were immune-labeled with a *cis*-Golgi marker (Figure 30). When we focused on the transfected cells with pDronpa-p24, the dronpa tagged p24 (green) colocalizes with GM130 (red). Since p24 protein is known to be mainly located in the Golgi area, this colocalization shows the correct localization of the recombinant protein.

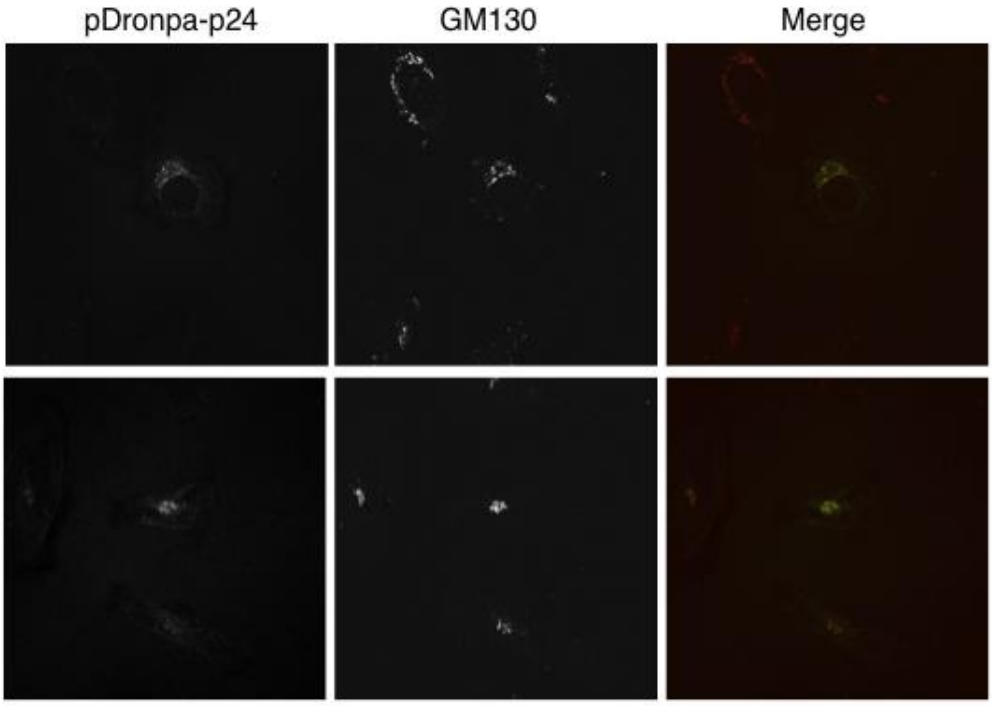

FIGURE 30: Colocalization of pDronpa-p24 with a *cis*-Golgi marker. HeLa cells transfected with pDronpa-p24 is labeled with a *cis*-Golgi marker. pDronpa-p24 (green), GM130 (red), colocalization (yellow).

Taken together, pDronpa-p24 construct was cloned and verified to localize properly at the perinuclear region.

4. Discussion

4.1. CHAPTER I: Role of γ2-COP in the transport of SH4 domain containing proteins

Here we investigated a potential specific role of either of the two γ subunits of coatomer in the unconventional transport of two reporter proteins by different cell lines. To study the role of γ2-COP in the transport of the SH4 domain containing HASPB and Yes proteins, stable cell lines were created and tested in biochemical and microscopy analysis.

Clathrin coated vesicles are responsible for trafficking in the late secretory pathway (*trans*-Golgi network, endosomes, lysosomes, plasma membrane) in eukaryotic cells are, and are often compared to the COPI system because of their structural analogy that has emerged due to a growing set of X-ray crystallographic structures of bits and pieces of such complexes (Popoff et al., 2011a; Robinson, 2004). Their coats consist of an outer layer (Clathrin heavy and light chains) and an inner layer (adaptor proteins). Similarly, the heptameric coatomer complex can be dissociated into tetrameric (β/δ/γ/ζ-COP) and trimeric (α/β'/ε-COP) subcomplexes. The tetrameric coatomer subcomplex shares similarities to the adaptor proteins of the clathrin coat, while the trimeric coatomer subcomplex is similar to the heavy and light chains of clathrin (Popoff et al., 2011a; Xing et al., 2010).

Furthermore, there are different adaptor complexes of the clathrin coat. These are located in different parts of the late secretory pathway and fulfill different functions (Robinson, 2004). In a similar way there are four different isoforms of coatomer, which are expressed in different amounts and located to different parts of the Golgi apparatus (Moelleken et al., 2007). It is highly likely for the different COPI isoforms to also exhibit different functions, similar to the many clathrin adaptor complexes known. Recently, a selectivity for cargo of the COPI isoforms has been investigated: Electron microscopy and biochemical studies

revealed compositionally distinct populations of COPI vesicles in *in vivo* and *in vitro* systems (Malsam et al., 2005; Orci et al., 1997).

Preliminary data from Nickel Laboratory showed that transport of HASPB (SH4-protein) is affected by down regulation of γ2-COP. Ritzerfeld et al. described that down regulation of β-COP in HeLa cell lines expressing both SH4-proteins results in retention of the HASPB in the perinuclear region while Yes was able to reach to plasma membrane. As stable cell lines expressing the SH4-proteins HASPB and Yes were available (Ritzerfeld et al., 2011), we extended our knockdown experiments to other coatomer subunits α, β, δ, ζ and especially to γ-COP to validate the preliminary data and to obtain more insights on the role of different subunits in the trafficking of SH4-proteins. siRNA knockdown experiments in mammalian cells show a reduction of the respective coatomer subunits (α, β, δ, ζ1-COP), which leads to a significant phenotype for one of the SH4-proteins: HASPB. However, knockdown of individual γ subunits did not affect transport of HASPB protein. Therefore, our data shows that transport of SH4-proteins to the plasma membrane is dependent on the coatomer complex, and therefore most likely on COPI vesicles. However, in the scope of this thesis, it could be shown that when one of the γ subunits was down regulated, the other subunits were sufficient to rescue the transport of the SH4-protein HASPB to the plasma membrane.

Furthermore, previously created stable cell lines expressing HA and myc tagged γ1-COP and γ2-COP (respectively) from Jörg Moelleken were used as a template. When the mouse fibroblast cell line 3T3 was characterized, unexpectedly, a down-regulation of the endogenous proteins was observed, while the exogenous γ-COP subunits were increased. This resulted in only one of the tagged γ-COP subunits being present in 3T3 cells after induction. Newly created cell lines are stably expressing the reporter proteins, which already carry a γ subunit knockdown system as the template 3T3 cells. The recombinant proteins were expressed in the new 3T3 cell lines and analyzed. However, again there was no different phenotype between γ subunits. This indicates that upon down regulation of one of the γ subunits, the other one was able to rescue transport of SH4-proteins to the plasma membrane. A possible

explanation for this might be that in case of a lack in the coatomer isoforms in cells, other isoforms can take initiative in the transport of this cargo to fulfill the task. However, this could also be interpreted by coatomer isoforms having no preference for transporting different SH4-proteins to the plasma membrane.

Knock down of the coatomer subunits also showed the absence of the ζ2 subunit in HeLa cells. Recently, analyses of ζ subunits existing in cancer cells versus normal cells opened up a new path for cancer therapeutics (Shtutman et al., 2011). Shtutman and colleagues showed different levels of the two ζ subunits in different cancer cell lines by qRT-PCR and revealed a possibility of targeting ζ1-COP for the treatment of the cancer cells. Our findings show a pronounced retention effect of ζ1 subunit knockdown in the transport of HASPB reporter protein. These results are consistent with the previous studies and suggest in a cell with only one copy of ζ subunit makes ζ1-COP indispensable. Taken together, the functions of the coatomer isoforms can be substituted by other isoforms in our cell culture system but this does not exclude that there are special circumstances where the presence of one subunit is vital for the organism. These might be special cell types, special cargo or special environmental conditions.

It appears that there is no significant role of γ2-COP in the plasma membrane localization of the SH4-proteins. However, in the scope of this thesis, only two SH4-proteins could be investigated. Clearly, this investigation should be extended to a variety of SH4-proteins and other proteins that carry different domains, ideally to a genome wide scale. The cell biological analysis could be combined with biochemical analyses and include cargo proteins with known preferences for one or the other γ subunit in future experiments. For example, in vitro experiments resulted in uptake differences of some cargo (MannosidaseII and GOLPH3) within the COPI vesicles generated from different coatomer isoforms (personal communication, Vincent Poppof, Britta Brügger, Felix Wieland).

It is also tempting to extend the analysis to a multitude of proteins of a given cell. This could be done for example by monitoring the levels of all cell surface

proteins in γ1 and γ2 knock downs compared to the wild type, by proteomic analysis of the pull-down of surface labeled (NHS-sulfo-Biotin) proteins or quantitative FRET analysis.

4.2. CHAPTER II: Impact of Brefeldin A analogues on Golgi morphology

Brefeldin A (BFA) is a unique fungal metabolite that has the unusual property of (reversibly) disassembling the structure of the Golgi apparatus (Lippincott-Schwartz et al., 1989). This causes a block of protein transport between the ER and the Golgi in eukaryotic cells (Fujiwara et al., 1988). In addition, BFA has an inhibitory effect on enterovirus replication (Cuconati et al., 1998) and an apoptotic effect on cancer cells (Seehafer et al., 2013; Shao et al., 1996).

In this chapter, effects of novel BFA analogues on mammalian cells were investigated. In comparison to the effect of BFA, two sets of newly synthesized analogues were tested at concentrations of 1 µg/ml and 5 µM and different times (30 min, 60 min, and 2 h wash-out after 60 min).

In a first batch 6 analogues were tested. Two of the six analogues were affecting the Golgi morphology, namely, (6R)-hydroxy-BFA and BFA lactam analogue. The BFA lactam analogue differed from the other compounds in an earlier start of Golgi reassembly, 60 min even before washout. This reassembly effect before washout is likely due to a metabolisation or secretion of the drugs (Bruning et al., 1992; Förster et al., 2011a). Treatment with all compounds of the second set showed an effect on the Golgi morphology similar to BFA. Once compounds were washed out, only the Golgi dissociation caused by derivative 39e turned out to be reversible, again similar to BFA. The other two compounds (39a and 39b) after wash out only partially allowed to regain the structure of the Golgi, while one of the compounds (5) did not at all allow recovery of the Golgi.

Although BFA itself is an important tool used in vesicular transport studies (Helms and Rothman, 1992b); it is also of interest for other fields of research,

e.g. it is a potential anti-cancer and anti-viral drug. The cytotoxic effect of BFA is known in various human cancer cells (Tseng et al., 2013). Tseng and colleagues performed cell culture experiments by determining the survival rate of the suspension and adhesion cultures under increasing amount of BFA treatment conditions and observed BFA-mediated suppression of the progress of colorectal cancer (one of the most common cancer types) during the stages of tumorogenesis and metastasis. Furthermore, the impact of BFA on androgen-mediated prostate cancer cell growth was investigated by focusing on the cell cycle and androgen receptor regulation by Rajamahanty and colleagues. They found BFA to exert a very strong growth inhibitory activity on androgen-mediated prostate cancer cell lines by cell cycle arrest and the down regulation of androgen receptor activity and expression (Rajamahanty et al., 2010). Another important effect of BFA is on the function in the entry of virus, their replication and assembly (van der Linden et al., 2010). For example, Dasgupta and Wilson showed that a primary effect of BFA on Herpes Simplex Virus type1 is an assembly defect, during formation of perinuclear enveloped virus particles at the inner nuclear membrane (Dasgupta and Wilson, 2001).

In the scope of this thesis, BFA analogues with different effects on Golgi disruption and reassembly in mammalian cells were analyzed that have great potential to be used in other fields. Unlike BFA, more stable, less toxic, not reversible etc. analogues could be useful as therapeutics. Based on these findings, it might be possible to develop new therapies for treatment of various cancers.

4.3. CHAPTER III: Oligomerization of p24 and p24L17F transmembrane domains

All members of the p24 family cycle within the early secretory pathway (Gommel et al., 2001; Jenne et al., 2002; Schuiki, 2012) as they are recognized via their cytoplasmic tails and transported by COPI and COPII vesicles (Dominguez et al., 1998; Schuiki, 2012; Sohn et al., 1996). In addition to their monomeric and dimeric forms, most p24 family members form heterooligomers

within the family, which is essential for their proper localization and stability (Jenne et al., 2002; Gommel et al., 1999). Recently, higher oligomeric forms of p24 were observed upon *in vivo* crosslinking (Contreras et al., 2012; this thesis). This is especially interesting as the biogenesis of COPI vesicle is initiated by the binding of the cytoplasmic tails of dimeric p24 proteins to Arf and then to the γ-COP (Gommel et al., 2001; Bethune et al., 2006; Zhao et al., 1999).

In addition to the oligomeric forms and the protein-protein interactions of the p24 family members, recent experiments revealed an interaction between p24 with a specific lipid. This interaction was not observed with the very closely related p23 protein (Contreras et al., 2012). The interaction of the transmembrane domain of p24 with a specific sphingolipid species (SM 18:0) was revealed by FRET experiments with fluorescent lipids. The oligomeric form of p24 and a non-SM18 binding p24 variant (L17F) were investigated *in vivo* as part of the thesis.

Optimization of the doxycycline induction resulted in the comparable amount of expression levels of the recombinant proteins. The recombinant p24 proteins were successfully cross-linked *in vivo* using a chemical crosslink agent. Quantification of *in vivo* crosslink experiments implies a significant reduction in the oligomeric forms to monomeric forms ratio of p24L17F. These data are a strong indication that the shift in equilibrium of p24 as found *in vitro* does also occur *in vivo*, and that SM 18 binding is of physiological importance. In accordance with the *in vitro* crosslinking data on transmembrane domains of p24, the specific interaction of sphingolipid (SM 18:0) with the transmembrane domain of p24 facilitates oligomerization of the p24 *in vivo* as well. This work was published in Contreras et al. (2012).

4.4. CHAPTER IV: Kinetics of the p24 family members

Members of the p24 family cycle between the membrane bound compartments of the early secretory pathway. Indications existed from earlier experiments,

that individual members of the family cycle at different rates. *In vivo* trafficking of fluorescently tagged p23 and p24 from the ERGIC to the Golgi could be examined by microscopy after temperature shifts and was estimated to move at 9.7 µm in 10 seconds in the average, with varying speeds (max. speed 1.6 µm/s) (Blum et al., 1999). In yeast, deletion of the p24 family members resulted in a reduction of the speed of ER to Golgi transport for a subset of secretory proteins (Denzel et al., 2000; Marzioch et al., 1999). In addition, immune fluorescent labeling revealed two distinct groups of p24 family members, distinguished by different travel rates from the Golgi to the ER (Eva Emig, PhD thesis).

In this thesis, in the anticipation to challenge the kinetics of the p24 family members, two proteins were investigated (p23 and p24). Detailed characterization of the cells expressing fluorescent-tagged (YFP) p23 and p24 proteins at hand was carried out.

Biochemical and microscopic analysis revealed heterogenic expression levels of the recombinant proteins, which were solved by Fluorescence Activated Cell Sorting (FACS) of the cells.

Golgi export kinetics of the p24 proteins were examined in comparison to the non-SM 18 binding p24 mutant (p24L17F) by FLIP. This showed a reduction in the half-life of Golgi-associated fluorescence of fluorescence-tagged p24 to 4.5 min (Contreras et al., 2012). Despite the fact that the cell morphologies were quite different, several trials of FLIP experiments were performed with the previously defined settings for HeLa cell lines. CHO cell lines are morphologically more elongated compared to HeLa cell lines. Setting up ROI's on the both sides of the Golgi area with a certain distance to protect the cell from unintended bleaching was not possible but for a few cells in hundreds. This obstacle could be overcome by adjusting the settings for these cell lines: the ROI size, number and/or location.

In the end, FLIP experiments were performed successfully with HeLa cell lines. Nevertheless, no significant differences were observed between transport rates

of p23 and p24 from Golgi to ER with these means, although in individual experiments such differences could be observed.

Another fluorescent protein tag with more advantages additional to those offered by YFP was introduced to p23 and p24 proteins as a fusion protein. It is a novel GFP-like protein with a photo-activatable feature, which was previously used for tracking of proteins *in vivo* (Andresen et al., 2007; Fujioka et al., 2006). Photoactivatable fluorescent proteins (PFAPs) are recently discovered, useful reporters of the dynamic behavior of proteins *in vivo* and a great tool for the microscopy of the kinetics of proteins in living cells (Day and Davidson, 2009; Lukyanov et al., 2005). Dronpa is the most prominent and well-studied member of the photoactivatable fluorescent proteins (Day and Davidson, 2009). To investigate the kinetics of p24 family members, p23 and p24 Dronpa fusion constructs were created. One of the dronpa constructs (pDronpa-p24) was produced successfully and analyzed biochemically and microscopically. However, pDronpa-p23 constructs did not yield stable recombinant protein according to *in vivo* and biochemical analysis. The predominantly cytosolic localization of the pDronpa-p23 construct *in vivo* is likely due to proteolytic truncation of the more stable Dronpa protein domain.

The Dronpa-tagged p24 protein family members can be activated at the location of interest and follow up their path throughout the cell, thereby obtaining protein transport rates. The cloning strategy for pDronpa-p23 will have to be altered and improved to achieve a more stable construct. If a stable clone of pDronpa-p23 was available, future experiments could provide further insights into the transport rates of p24 family members. Eventually, such experiments should be extended to other members of the p24 family.

5. Appendix

5.1. Abbreviations

3T3g1	3T3/rtTA-HA-hγ1
3T3g2	3T3/rtTA-Myc-hγ2
ADP	Adenosine diphosphate
Arf1	ADP-ribosylation factor 1
BFA	Brefeldin A
BSA	Bovine serum albumin
C	Centigrade
C-terminal	carboxy-terminal
CHO	Chinese hamster ovary
COP	Coat Protein
DMEM	Dulbecco’s Modified Eagle's Medium
DMSO	Dimethyl sulfoxide
DNA	Deoxyribonucleic acid
dNTP	Deoxyribonucleotide triphosphates
DSG	Disuccinimidyl glutarate
E. coli	Escherichia coli
EDTA	Ethylenediaminetetraacetic acid
ER	Endoplasmic Reticulum
ERGIC	Endoplasmic Reticulum-Golgi Intermediate Compartment
FACS	Fluorescence-activated cell sorting
FBS	Fetal Bovine Serum
FCS	Fetal Calf Serum
FGF	Fibroblast growth factor
FLIP	Fluorescence Loss in Photobleaching
FSC	Forward scatter
GAPDH	Glyceraldehyde 3-phosphate dehydrogenase
GBF1	Golgi-specific Brefeldin A resistant guanine nucleotide exchange factor 1
GDP	Guanosin diphosphate
GEF	Guanine Exchange Factor
GFP	Green Fluorescent Protein
GPI	Glycosylphosphatidylinositol
GTP	Guanosin triphosphate
h	Hour(s)
HASPB	Hydrophilic Acylated Surface Protein B
HEK	Human Embryonic Kidney
HeLa double5	HeLa SH4-HASPBN18-GFP/SH4-YesN18-Cherry Clone#5
IgG	immunoglobulin G
IP	immunoprecipitation
kb	kilo base pairs
kDa	kilo-Dalton

LB	Luria Broth
LSM	Laser Scanning Microscopy
min	Minute(s)
MW	Molecular Weight
N-terminal	Amino terminal
PAGE	Polyacrylamide gel electrophoresis
PBS	Phosphate buffered saline
PCR	Polymerase chain reaction
PVDF	Polyvinylidene difluoride
qRT-PCR	Quantitative real time PCR
ROI	Region(s) of Interest
rpm	Revolutions per minute
SDS	Sodium dodecyl sulfate
sec	Second(s)
siRNA	Small interfering RNA
TEMED	N, N, N', N'-Tetramethylethylenediamine
V	Volt
wt	wild type
YFP	Yellow Fluorescent Protein
α	Alpha
β	Beta
β'	Beta prime
γ	Gamma
δ	Delta
ε	Epsilon
ζ	Zeta

5.2. List of Publications

Synthesis and Biological Properties of Novel Brefeldin A Analogues. Kai Seehafer, Frank Rominger, Günter Helmchen, Markus Langhans, David G. Robinson, Başak Özata, Britta Brügger, Jeroen R. P. M. Strating, Frank J. M. van Kuppeveld, and Christian D. Klein. ***J. Med. Chem.,*** **2013**, 56 (14), 5872–5884.

Molecular recognition of a single sphingolipid species by a protein's transmembrane domain. F.-Xabier Contreras, Andreas M. Ernst, Per Haberkant, Patrik Björkholm, Erik Lindahl, Başak Gönen, Christian Tischer, Arne Elofsson, Gunnar von Heijne, Christoph Thiele, Rainer Pepperkok, Felix Wieland & Britta Brügger. Nature, 2012, 481, 525-529.

Syntheses and Biological Properties of Brefeldin Analogues. Sebastian Förster, Elke Persch, Olena Tverskoy, Frank Rominger, Günter Helmchen, Christian Klein, Basak Gönen, and Britta Brügger. ***Eur. J. Org. Chem.,*** **2011**, 878–891.

5.3. References

Aguilera-Romero, A., Kaminska, J., Spang, A., Riezman, H., and Muniz, M. (2008). The yeast p24 complex is required for the formation of COPI retrograde transport vesicles from the Golgi apparatus. The Journal of cell biology *180*, 713-720.

Andresen, M., Stiel, A.C., Trowitzsch, S., Weber, G., Eggeling, C., Wahl, M.C., Hell, S.W., and Jakobs, S. (2007). Structural basis for reversible photoswitching in Dronpa. Proceedings of the National Academy of Sciences of the United States of America *104*, 13005-13009.

Antonny, B., Beraud-Dufour, S., Chardin, P., and Chabre, M. (1997). N-terminal hydrophobic residues of the G-protein ADP-ribosylation factor-1 insert into membrane phospholipids upon GDP to GTP exchange. Biochemistry *36*, 4675-4684.

Beck, R., Sun, Z., Adolf, F., Rutz, C., Bassler, J., Wild, K., Sinning, I., Hurt, E., Brugger, B., Bethune, J.*, et al.* (2008). Membrane curvature induced by Arf1-GTP is essential for vesicle formation. Proceedings of the National Academy of Sciences of the United States of America *105*, 11731-11736.

Beller, M., Sztalryd, C., Southall, N., Bell, M., Jäckle, H., Auld, S.D., and Oliver, B. (2008). COPI Complex Is a Regulator of Lipid Homeostasis. PLOS biology *6*, 2530-2549.

Berger, E.G., Grimm, K., Bachi, T., Bosshart, H., Kleene, R., and Watzele, M. (1993). Double immunofluorescent staining of alpha 2,6 sialyltransferase and beta 1,4 galactosyltransferase in monensin-treated cells: evidence for different Golgi compartments? Journal of cellular biochemistry *52*, 275-288.

Bethune, J., Wieland, F., and Moelleken, J. (2006). COPI-mediated transport. The Journal of membrane biology *211*, 65-79.

Blum, R., Pfeiffer, F., Feick, P., Nastainczyk, W., Kohler, B., Schafer, K.H., and Schulz, I. (1999). Intracellular localization and in vivo trafficking of p24A and p23. Journal of cell science *112 (Pt 4)*, 537-548.

Bonifacino, J.S., and Glick, B.S. (2004). The mechanisms of vesicle budding and fusion. Cell *116*, 153-166.

Bonnon, C., Wendeler, M.W., Paccaud, J.P., and Hauri, H.P. (2010). Selective export of human GPI-anchored proteins from the endoplasmic reticulum. Journal of cell science *123*, 1705-1715.

Bruning, A., Ishikawa, T., Kneusel, R.E., Matern, U., Lottspeich, F., and Wieland, F.T. (1992). Brefeldin A binds to glutathione S-transferase and is secreted as glutathione and cysteine conjugates by Chinese hamster ovary cells. The Journal of biological chemistry *267*, 7726-7732.

Buechling, T., Chaudhary, V., Spirohn, K., Weiss, M., and Boutros, M. (2011). p24 proteins are required for secretion of Wnt ligands. EMBO reports *12*, 1265-1272.

Campbell, J.L., and Schekman, R. (1997). Selective packaging of cargo molecules into endoplasmic reticulum-derived COPII vesicles. Proceedings of the National Academy of Sciences of the United States of America *94*, 837-842.

Casanova, J.E. (2007). Regulation of Arf Activation: the Sec7 Family of Guanine Nucleotide Exchange Factors. Traffic *8*, 1476–1485.

Claude, A., Zhao, B.P., Kuziemsky, C.E., Dahan, S., Berger, S.J., Yan, J.P., Armold, A.D., Sullivan, E.M., and Melancon, P. (1999). GBF1: A novel Golgi-

associated BFA-resistant guanine nucleotide exchange factor that displays specificity for ADP-ribosylation factor 5. The Journal of cell biology *146*, 71-84.
Contreras, F.X., Ernst, A.M., Haberkant, P., Bjorkholm, P., Lindahl, E., Gonen, B., Tischer, C., Elofsson, A., von Heijne, G., Thiele, C.*, et al.* (2012). Molecular recognition of a single sphingolipid species by a protein's transmembrane domain. Nature *481*, 525-529.
Cottom, N.P., and Ungar, D. (2012). Retrograde vesicle transport in the Golgi. Protoplasma *249*, 943–955.
Cuconati, A., Molla, A., and Wimmer, E. (1998). Brefeldin A inhibits cell-free, de novo synthesis of poliovirus. Journal of virology *72*, 6456-6464.
D'Souza-Schorey (2006). ARF proteins: roles in membrane traffic and beyond. Nature Reviews *7*.
Dancourt, J., and Barlowe, C. (2010). Protein sorting receptors in the early secretory pathway. Annu Rev Biochem *79*, 777-802.
Dasgupta, A., and Wilson, D.W. (2001). Evaluation of the primary effect of brefeldin A treatment upon herpes simplex virus assembly. The Journal of general virology *82*, 1561-1567.
Day, R.N., and Davidson, M.W. (2009). The fluorescent protein palette: tools for cellular imaging. Chem Soc Rev *38*, 2887-2921.
Denzel, A., Otto, F., Girod, A., Pepperkok, R., Watson, R., Rosewell, I., Bergeron, J.J., Solari, R.C., and Owen, M.J. (2000). The p24 family member p23 is required for early embryonic development. Current biology : CB *10*, 55-58.
Dominguez, M., Dejgaard, K., Fullekrug, J., Dahan, S., Fazel, A., Paccaud, J.P., Thomas, D.Y., Bergeron, J.J., and Nilsson, T. (1998). gp25L/emp24/p24 protein family members of the cis-Golgi network bind both COP I and II coatomer. The Journal of cell biology *140*, 751-765.
Donaldson, J.G., Finazzi, D., and Klausner, R.D. (1992). Brefeldin A inhibits Golgi membrane-catalysed exchange of guanine nucleotide onto ARF protein. Nature *360*, 350-352.
Emery, G., Rojo, M., and Gruenberg, J. (2000). Coupled transport of p24 family members. Journal of cell science *113 (Pt 13)*, 2507-2516.
Eugster, A., Frigerio, G., Dale, M., and Duden, R. (2000). COP I domains required for coatomer integrity, and novel interactions with ARF and ARF-GAP. The EMBO journal *19*, 3905-3917.
Farhan, H., and Rabouille, C. (2011). Signalling to and from the secretory pathway. Journal of cell science *124*, 171-180.
Fiedler, K., and Rothman, J.E. (1997). Sorting determinants in the transmembrane domain of p24 proteins. The Journal of biological chemistry *272*, 24739-24742.
Fiedler, K., Veit, M., Stamnes, M.A., and Rothman, J.E. (1996). Bimodal Interaction of Coatomer with the p24 Family of Putative Cargo Receptors. Science *273*.
Förster, S., Persch, E., Tverskoy, O., Rominger, F., Helmchen, G., Klein, C., Gönen, B., and Brügger, B. (2011a). Syntheses and Biological Properties of Brefeldin Analogues. Eur J Org Chem *2011*, 878–891.
Förster, S., Persch, E., Tverskoy, O., Rominger, F., Helmchen, G., Klein, C., Gönen, B., and Brügger, B. (2011b). Syntheses and Biological Properties of Brefeldin Analogues. European Journal of Organic Chemistry *2011*, 878-891.

Fujioka, A., Terai, K., Itoh, R.E., Aoki, K., Nakamura, T., Kuroda, S., Nishida, E., and Matsuda, M. (2006). Dynamics of the Ras/ERK MAPK cascade as monitored by fluorescent probes. The Journal of biological chemistry *281*, 8917-8926.
Fujiwara, T., Oda, K., Yokota, S., Takatsuki, A., and Ikehara, Y. (1988). Brefeldin A causes disassembly of the Golgi complex and accumulation of secretory proteins in the endoplasmic reticulum. The Journal of biological chemistry *263*, 18545-18552.
Fullekrug, J., Suganuma, T., Tang, B.L., Hong, W., Storrie, B., and Nilsson, T. (1999). Localization and recycling of gp27 (hp24gamma3): complex formation with other p24 family members. Molecular biology of the cell *10*, 1939-1955.
Futatsumori, M., Kasai, K., Takatsu, H., Shin, H., and Nakayama, K. (2000). Identification and Characterization of Novel Isoforms of COP I Subunits. J Biochem *128*, 793-801.
Gommel, D., Orci, L., Emig, E.M., Hannah, M.J., Ravazzola, M., Nickel, W., Helms, J.B., Wieland, F., and Sohn, K. (1999). p24 and p23, the major transmembrane proteins of COPI-coated transport vesicles, form hetero-oligomeric complexes and cycle between the organelles of the early secretory pathway. FEBS Letters *447*, 179-185.
Gommel, D.U., Memon, A.R., Heiss, A., Lottspeich, F., Pfannstiel, J., Lechner, J., Reinhard, C., Helms, J.B., Nickel, W., and Wieland, F.T. (2001). Recruitment to Golgi membranes of ADP-ribosylation factor 1 is mediated by the cytoplasmic domain of p23. The EMBO journal *20*, 6751-6760.
Hara-Kuge, S., Kuge, O., Orci, L., Amherdt, M., Ravazzola, M., Wieland, F.T., and Rothman, J.E. (1994). En bloc incorporation of coatomer subunits during the assembly of COP-coated vesicles. J Cell Biol *124*, 883-892.
Harter, C., and Wieland, F.T. (1998). A single binding site for dilysine retrieval motifs and p23 within the gamma subunit of coatomer. Proceedings of the National Academy of Sciences of the United States of America *95*, 11649-11654.
Helms, and Rothman (1992a). Inhibition by brefeldin A of a Golgi membrane enzymethat catalyses exchange of guanine nucleotide bind to Arf. Nature *360*.
Helms, J.B., and Rothman, J.E. (1992b). Inhibition by brefeldin A of a Golgi membrane enzyme that catalyses exchange of guanine nucleotide bound to ARF. Nature *360*, 352-354.
Hicke, L., Yoshihisa, T., and Schekman, R. (1992). Sec23p and a novel 105-kDa protein function as a multimeric complex to promote vesicle budding and protein transport from the endoplasmic reticulum. Molecular biology of the cell *3*, 667-676.
Hirschberg, K., and Lippincott-Schwartz, J. (1999). Secretory pathway kinetics and in vivo analysis of protein traffic from the Golgi complex to the cell surface. FASEB J *13 Suppl 2*, S251-256.
Jenne, N., Frey, K., Brugger, B., and Wieland, F.T. (2002). Oligomeric state and stoichiometry of p24 proteins in the early secretory pathway. The Journal of biological chemistry *277*, 46504-46511.
Jerome-Majewska, L.A., Achkar, T., Luo, L., Lupu, F., and Lacy, E. (2010). The trafficking protein Tmed2/p24beta(1) is required for morphogenesis of the mouse embryo and placenta. Developmental biology *341*, 154-166.

Klausner, R.D., Donaldson, J.G., and Lippincott-Schwartz, J. (1992). Brefeldin A: insights into the control of membrane traffic and organelle structure. The Journal of cell biology *116*, 1071-1080.
Lavieu, G., Orci, L., Shi, L., Geiling, M., Ravazzola, M., Wieland, F., Cosson, P., and Rothman, J.E. (2010). Induction of cortical endoplasmic reticulum by dimerization of a coatomer-binding peptide anchored to endoplasmic reticulum membranes. Proceedings of the National Academy of Sciences of the United States of America *107*, 6876-6881.
Lavoie, C., Paiement, J., Dominguez, M., Roy, L., Dahan, S., Gushue, J.N., and Bergeron, J.J. (1999). Roles for alpha(2)p24 and COPI in endoplasmic reticulum cargo exit site formation. The Journal of cell biology *146*, 285-299.
Lee, M.C., Miller, E.A., Goldberg, J., Orci, L., and Schekman, R. (2004). Bi-directional protein transport between the ER and Golgi. Annual review of cell and developmental biology *20*, 87-123.
Lippincott-Schwartz, J., Donaldson, J.G., Schweizer, A., Berger, E.G., Hauri, H.P., Yuan, L.C., and Klausner, R.D. (1990). Microtubule-dependent retrograde transport of proteins into the ER in the presence of brefeldin A suggests an ER recycling pathway. Cell *60*, 821-836.
Lippincott-Schwartz, J., and Liu, W. (2006). Insights into COPI coat assembly and function in living cells. Trends in cell biology *16*, e1-4.
Lippincott-Schwartz, J., Yuan, L.C., Bonifacino, J.S., and Klausner, R.D. (1989). Rapid redistribution of Golgi proteins into the ER in cells treated with brefeldin A: evidence for membrane cycling from Golgi to ER. Cell *56*, 801-813.
Lukyanov, K.A., Chudakov, D.M., Lukyanov, S., and Verkhusha, V.V. (2005). Innovation: Photoactivatable fluorescent proteins. Nature reviews Molecular cell biology *6*, 885-891.
Majoul, I., Straub, M., Hell, S.W., Duden, R., and Soling, H.D. (2001). KDEL-cargo regulates interactions between proteins involved in COPI vesicle traffic: measurements in living cells using FRET. Developmental cell *1*, 139-153.
Malsam, J., Satoh, A., Pelletier, L., and Warren, G. (2005). Golgin tethers define subpopulations of COPI vesicles. Science *307*, 1095-1098.
Marzioch, M., Henthorn, D.C., Herrmann, J.M., Wilson, R., Thomas, D.Y., Bergeron, J.J., Solari, R.C., and Rowley, A. (1999). Erp1p and Erp2p, partners for Emp24p and Erv25p in a yeast p24 complex. Molecular biology of the cell *10*, 1923-1938.
Matsuoka, K., Orci, L., Amherdt, M., Bednarek, S.Y., Hamamoto, S., Schekman, R., and Yeung, T. (1998). COPII-coated vesicle formation reconstituted with purified coat proteins and chemically defined liposomes. Cell *93*, 263-275.
Mitrovic, S., Ben-Tekaya, H., Koegler, E., Gruenberg, J., and Hauri, H.P. (2008). The cargo receptors Surf4, endoplasmic reticulum-Golgi intermediate compartment (ERGIC)-53, and p25 are required to maintain the architecture of ERGIC and Golgi. Molecular biology of the cell *19*, 1976-1990.
Moelleken, J., Malsam, J., Betts, M.J., Movafeghi, A., Reckmann, I., Meissner, I., Hellwig, A., Russell, R.B., Sollner, T., Brugger, B.*, et al.* (2007). Differential localization of coatomer complex isoforms within the Golgi apparatus. Proceedings of the National Academy of Sciences of the United States of America *104*, 4425-4430.

Nakano, R.T., Matsushima, R., Ueda, H., Tamura, K., Shimada, T., Li, L., Hayashi, Y., Kondo, M., Nishimura, M., and Hara-Nishimura, I. (2009). GNOM-LIKE1/ERMO1 and SEC24a/ERMO2 are required for maintenance of endoplasmic reticulum morphology in Arabidopsis thaliana. The Plant cell *21*, 3672-3685.
Nickel, W. (2010). Pathways of unconventional protein secretion. Current opinion in biotechnology *21*, 621-626.
Nickel, W., Sohn, K., Bunning, C., and Wieland, F.T. (1997). p23, a major COPI-vesicle membrane protein, constitutively cycles through the early secretory pathway. Proceedings of the National Academy of Sciences of the United States of America *94*, 11393-11398.
Niu, T.K., Pfeifer, A.C., Lippincott-Schwartz, J., and Jackson, C.L. (2005). Dynamics of GBF1, a Brefeldin A-sensitive Arf1 exchange factor at the Golgi. Molecular biology of the cell *16*, 1213-1222.
Orci, L., Stamnes, M., Ravazzola, M., Amherdt, M., Perrelet, A., Sollner, T.H., and Rothman, J.E. (1997). Bidirectional transport by distinct populations of COPI-coated vesicles. Cell *90*, 335-349.
Peyroche, A., Antonny, B., Robineau, S., Acker, J., Cherfils, J., and Jackson, C.L. (1999). Brefeldin A Acts to Stabilize an Abortive ARF–GDP–Sec7 Domain Protein Complex: Involvement of Specific Residues of the Sec7 Domain. Molecular Cell *3*, 275–285.
Phair, R.D., and Misteli, T. (2001). Kinetic modelling approaches to in vivo imaging. Nature reviews Molecular cell biology *2*, 898-907.
Popoff, V., Adolf, F., Brugger, B., and Wieland, F. (2011a). COPI budding within the Golgi stack. Cold Spring Harbor perspectives in biology *3*, a005231.
Popoff, V., Langer, J.D., Reckmann, I., Hellwig, A., Kahn, R.A., Brugger, B., and Wieland, F.T. (2011b). Several ADP-ribosylation factor (Arf) isoforms support COPI vesicle formation. The Journal of biological chemistry *286*, 35634-35642.
Rabouille, C., Malhotra, V., and Nickel, W. (2012). Diversity in unconventional protein secretion. Journal of cell science *125*, 5251-5255.
Reinhard, C., Harter, C., Bremser, M., Brugger, B., Sohn, K., Helms, J.B., and Wieland, F. (1999). Receptor-induced polymerization of coatomer. Proceedings of the National Academy of Sciences of the United States of America *96*, 1224-1228.
Ritzerfeld, J., Remmele, S., Wang, T., Temmerman, K., Brugger, B., Wegehingel, S., Tournaviti, S., Strating, J.R., Wieland, F.T., Neumann, B.*, et al.* (2011). Phenotypic profiling of the human genome reveals gene products involved in plasma membrane targeting of SRC kinases. Genome research *21*, 1955-1968.
Robinson, M.S. (2004). Adaptable adaptors for coated vesicles. Trends in cell biology *14*, 167-174.
Rojo, M., Emery, G., Marjomaki, V., McDowall, A.W., Parton, R.G., and Gruenberg, J. (2000). The transmembrane protein p23 contributes to the organization of the Golgi apparatus. Journal of cell science *113 (Pt 6)*, 1043-1057.
Rothman, J.E., and Wieland, F.T. (1996). Protein sorting by transport vesicles. Science *272*, 227-234.

Salama, N.R., Yeung, T., and Schekman, R.W. (1993). The Sec13p complex and reconstitution of vesicle budding from the ER with purified cytosolic proteins. The EMBO journal *12*, 4073-4082.
Sato, K. (2004). COPII coat assembly and selective export from the endoplasmic reticulum. Journal of biochemistry *136*, 755-760.
Schimmoller, F., Singer-Kruger, B., Schroder, S., Kruger, U., Barlowe, C., and Riezman, H. (1995). The absence of Emp24p, a component of ER-derived COPII-coated vesicles, causes a defect in transport of selected proteins to the Golgi. The EMBO journal *14*, 1329-1339.
Schuiki, I.a.V., A. (2012). Diverse roles for the p24 family of proteins in eukaryotic cells. BioMolecular Concepts *3*, 561–570.
Seehafer, K., Rominger, F., Helmchen, G., Langhans, M., Robinson, D.G., Ozata, B., Brugger, B., Strating, J.R., van Kuppeveld, F.J., and Klein, C.D. (2013). Synthesis and Biological Properties of Novel Brefeldin A Analogues. Journal of medicinal chemistry.
Serafini, T., Orci, L., Amherdt, M., Brunner, M., Kahn, R.A., and Rothman, J.E. (1991a). ADP-ribosylation factor is a subunit of the coat of Golgi-derived COP-coated vesicles: a novel role for a GTP-binding protein. Cell *67*, 239-253.
Serafini, T., Stenbeck, G., Brecht, A., Lottspeich, F., Orci, L., Rothman, J.E., and Wieland, F.T. (1991b). A coat subunit of Golgi-derived non-clathrin-coated vesicles with homology to the clathrin-coated vesicle coat protein beta-adaptin. Nature *349*, 215-220.
Shao, R.G., Shimizu, T., and Pommier, Y. (1996). Brefeldin A is a potent inducer of apoptosis in human cancer cells independently of p53. Experimental cell research *227*, 190-196.
Shtutman, M., Baig, M., Levina, E., Hurteau, G., Lim, C.U., Broude, E., Nikiforov, M., Harkins, T.T., Carmack, C.S., Ding, Y.*, et al.* (2011). Tumor-specific silencing of COPZ2 gene encoding coatomer protein complex subunit zeta 2 renders tumor cells dependent on its paralogous gene COPZ1. Proceedings of the National Academy of Sciences of the United States of America *108*, 12449-12454.
Sohn, K., Orci, L., Ravazzola, M., Amherdt, M., Bremser, M., Lottspeich, F., Fiedler, K., Helms, J.B., and Wieland, F.T. (1996). A major transmembrane protein of Golgi-derived COPI-coated vesicles involved in coatomer binding. The Journal of cell biology *135*, 1239-1248.
Soni, K.G., Mardones, G.A., Sougrat, R., Smirnova, E., Jackson, C.L., and Bonifacino, J.S. (2009). Coatomer-dependent protein delivery to lipid droplets. Journal of cell science *122*, 1834-1841.
Stenbeck, G., Harter, C., Brecht, A., Herrmann, D., Lottspeich, F., Orci, L., and Wieland, F.T. (1993). beta'-COP, a novel subunit of coatomer. The EMBO journal *12*, 2841-2845.
Strating, J.R., van Bakel, N.H., Leunissen, J.A., and Martens, G.J. (2009). A comprehensive overview of the vertebrate p24 family: identification of a novel tissue-specifically expressed member. Mol Biol Evol *26*, 1707-1714.
Sun, Z., Anderl, F., Frohlich, K., Zhao, L., Hanke, S., Brugger, B., Wieland, F., and Bethune, J. (2007). Multiple and stepwise interactions between coatomer and ADP-ribosylation factor-1 (Arf1)-GTP. Traffic *8*, 582-593.
Szul, T., and Sztul, E. (2011). COPII and COPI traffic at the ER-Golgi interface. Physiology (Bethesda) *26*, 348-364.

Takida, S., Maeda, Y., and Kinoshita, T. (2008). Mammalian GPI-anchored proteins require p24 proteins for their efficient transport from the ER to the plasma membrane. Biochem J *409*, 555-562.
Tournaviti, S., Hannemann, S., Terjung, S., Kitzing, T.M., Stegmayer, C., Ritzerfeld, J., Walther, P., Grosse, R., Nickel, W., and Fackler, O.T. (2007). SH4-domain-induced plasma membrane dynamization promotes bleb-associated cell motility. Journal of cell science *120*, 3820-3829.
Tseng, C.N., Huang, C.F., Cho, C.L., Chang, H.W., Huang, C.W., Chiu, C.C., and Chang, Y.F. (2013). Brefeldin a effectively inhibits cancer stem cell-like properties and mmp-9 activity in human colorectal cancer colo 205 cells. Molecules *18*, 10242-10253.
van der Linden, L., van der Schaar, H.M., Lanke, K.H., Neyts, J., and van Kuppeveld, F.J. (2010). Differential effects of the putative GBF1 inhibitors Golgicide A and AG1478 on enterovirus replication. Journal of virology *84*, 7535-7542.
Waters, M.G., Serafini, T., and Rothman, J.E. (1991). 'Coatomer': a cytosolic protein complex containing subunits of non-clathrin-coated Golgi transport vesicles. Nature *349*, 248-251.
Wiedler, M., Reinhard, C., Friedrich, G., Wieland, F., and Rösch, P. (2000). Structure of the Cytoplasmic Domain of p23 in Solution: Implications for the Formation of COPI Vesicles. Biochemical and Biophysical Research Communications *271*, 401–408.
Xing, Y., Bocking, T., Wolf, M., Grigorieff, N., Kirchhausen, T., and Harrison, S.C. (2010). Structure of clathrin coat with bound Hsc70 and auxilin: mechanism of Hsc70-facilitated disassembly. The EMBO journal *29*, 655-665.
Zanetti, G., Pahuja, K.B., Studer, S., Shim, S., and Schekman, R. (2012). COPII and the regulation of protein sorting in mammals. Nature cell biology *14*, 20-28.
Zhao, L., Helms, J.B., Brugger, B., Harter, C., Martoglio, B., Graf, R., Brunner, J., and Wieland, F.T. (1997). Direct and GTP-dependent interaction of ADP ribosylation factor 1 with coatomer subunit beta. Proceedings of the National Academy of Sciences of the United States of America *94*, 4418-4423.
Zhao, L., Helms, J.B., Brunner, J., and Wieland, F.T. (1999). GTP-dependent binding of ADP-ribosylation factor to coatomer in close proximity to the binding site for dilysine retrieval motifs and p23. The Journal of biological chemistry *274*, 14198-14203.

Acknowledgement

The contributions of many different people, in their different ways, have made this work possible. I want to thank everybody who contributed to the completion of this study.

There are no words to convey my deep gratitude and great respect for my advisor, Professor Felix Wieland, who not only gave me the opportunity to work in his lab, but also supported me with his excellent guidance, understanding, patience, and encouragement. I learned a lot.

I owe a great debt of gratitude to Britta Brügger, who was incredibly supportive on both an academic and a personal level. This thesis would not have been possible without her valuable advice, constructive criticism, and extensive discussions, for which I am extremely grateful. I am also in debt to Walter Nickel for passing me on an interesting project and his support during my study.

My sincere thanks must also go to the members of my exam committee: Walter Nickel, Thomas Söllner, and Hans Michael Müller. They generously offered their time.

I am sincerely grateful to Mathias, Andreas, Martin, and Weiwei. Their contributions made a significant difference to the overall shape of the dissertation.

I would like to thank all the previous and current colleagues for making the journey more challenging and fun scientifically and socially. Additionally I would like to thank Nickel lab members for sharing the floor, their friendships and equipment, which I needed at last minutes. Especially to Xabi for his patience and support, Andreas for scientific discussions and sharing the dark side with me, Mathias for his helpful scientific input and spreading positive energy, Koen for his help at the beginning with great patience, Julia for her collaboration and indispensable friendship, Simone for being my apple/orange as well as a fun lab-mate and a good friend, Rainer for his warm welcome, Jeroen for sharing different point of views on many subjects, Gabi and Sabine for their answers to my endless questions, Tao for handing over me the project with already a lot of progress, Iva for her help and nice chats, Timo for his friendship, and Çağakan for being a little brother to me, even though I don’t want one.

My sincere thanks go to my true friend, my dear Schmeisi. I don’t think I could have survived this journey without you Verena. I would like to thank to my great friend Martin for being tough competitor on almost every subject and for his valuable scientific input. I also thank Linda and Sonja for fun times at “girls’ night out” events.

Special thanks to little sun shines Annie, Mavie, Theo and Marie.

I am truly in debt to my dearest friend, my sister Sevda. Ups and downs of life is more bearable and more joyful with you. Always better to have someone

walking together on the same path and I was not alone. I am deeply thankful to my cousin Zeynep for making our life absurd and unnecessarily fun.

I wish to thank to Nuran, Handan, Mete, Shun Sr., Olivia, Selma and Shun Jr. for making me feel home here in Germany.

Finally, I must of course thank my beloved family for their loving considerations and great confidence beyond measure. My mother, Nesrin Gönen, who inspired me, my father, Taner Gönen, who never said “I miss you” even though he did and my brother, M. Ruhi Gönen, who helped me to make the first step. To them, I am eternally grateful. I also thank my mother-in-law Füsun Özata, and my grandma-in-law Meliha Canıtez for their great moral support and sacrifices.

This last word of acknowledgment I have saved for my love, Özgen Özata, who have been the inspiration and motivation in my life. I am very grateful for his unconditional love, encouragement, tolerance and support. Thank you for keeping me sane over the past few months and thank you for being my editor, proofreader, and sounding board. But most of all, thank you for being my best friend. I owe you everything.